SOUTHERN PLAINS
TRANSPORTATION CENTER

Tangential Heave Stress acting on Deep Foundations in Cold Regions

Hoyoung Seo, Ph.D., P.E.
Liang Li, Graduate Research Assistant
William D. Lawson, P.E., Ph.D.
Priyantha W. Jayawickrama, Ph.D.

SPTC15.1-17-F

Southern Plains Transportation Center
201 Stephenson Parkway, Suite 4200
The University of Oklahoma
Norman, Oklahoma 73019

DISCLAIMER

The contents of this report reflect the views of the authors, who are responsible for the facts and accuracy of the information presented herein. This document is disseminated under the sponsorship of the Department of Transportation University Transportation Centers Program, in the interest of information exchange. The U.S. Government assumes no liability for the contents or use thereof.

TECHNICAL REPORT DOCUMENTATION PAGE

1. REPORT NO.	2. GOVERNMENT ACCESSION NO.	3. RECIPIENTS CATALOG NO.
SPTC15.1-17-F		

4. TITLE AND SUBTITLE	5. REPORT DATE
Tangential Heave Stress Acting on Deep Foundations in Cold Regions	May 01 2019
	6. PERFORMING ORGANIZATION CODE
7. AUTHOR(S)	8. PERFORMING ORGANIZATION REPORT
Hoyoung Seo, Liang Li, William D. Lawson, and Priyantha W. Jayawickrama	
9. PERFORMING ORGANIZATION NAME AND ADDRESS	10. WORK UNIT NO.
Texas Tech Center for Multidisciplinary Research in Transportation Texas Tech University Box 41023 Lubbock, Texas 79409	11. CONTRACT OR GRANT NO. DTRT13-G-UTC36
12. SPONSORING AGENCY NAME AND ADDRESS	13. TYPE OF REPORT AND PERIOD COVERED
Southern Plains Transportation Center 201 Stephenson Pkwy, Suite 4200 The University of Oklahoma Norman, OK 73019	Final June 2016 – May 2019
	14. SPONSORING AGENCY CODE

15. SUPPLEMENTARY NOTES

University Transportation Center

16. ABSTRACT

In this study, the research team performed an experimental investigation of the effect of frost heave during soil freezing on the development of tangential heave force acting on deep foundations. A novel, laboratory-scale tangential heave testing system, instrumented with a model pile, moisture sensors and thermocouples, was developed in this study. The model pile was specially manufactured by bonding two vertically-cut half piles into a single, closed ended pipe pile and instrumented with strain gages and thermocouples on inner surface of the pile.

The test soil was subjected to a temperature gradient of 0.082°C/mm between the top (-10 °C) and bottom (15 °C) of the soil sample in an environmental chamber. The maximum heave amounts at the center and corner of the soil surface were about 18 mm and 14 mm, respectively. The pile top reached a peak upward movement of 0.533 mm at 24 hours, and no significant change was observed thereafter. The tangential heave stress measured in this study varied from about 66 kPa to 280 kPa. The tangential heave tests using the instrumented model pile and image acquisition system provided a wealth of information that can improve fundamental understanding of ice-soil-pile interaction. Furthermore, the testing system and procedure developed in this study may contribute to establish a test standard for tangential heave testing.

17. KEY WORDS	18. DISTRIBUTION STATEMENT
Tangential heave test; Deep foundations; Frost heave; Cold regions engineering	No restrictions. This publication is available at www.sptc.org and from the NTIS.

19. SECURITY CLASSIF. (OF THIS REPORT)	20. SECURITY CLASSIF. (OF THIS PAGE)	21. NO. OF PAGES	22. PRICE
Unclassified	Unclassified	76	

SI* (MODERN METRIC) CONVERSION FACTORS

APPROXIMATE CONVERSIONS TO SI UNITS

SYMBOL	WHEN YOU KNOW	MULTIPLY BY	TO FIND	SYMBOL
		LENGTH		
in	inches	25.4	millimeters	Mm
ft	feet	0.305	meters	m
yd	yards	0.914	meters	m
mi	miles	1.61	kilometers	km
		AREA		
in^2	square inches	645.2	square millimeters	mm^2
ft^2	square feet	0.093	square meters	m^2
yd^2	square yard	0.836	square meters	m^2
ac	acres	0.405	hectares	ha
mi^2	square miles	2.59	square kilometers	km^2
		VOLUME		
fl	fluid ounces	29.57	milliliters	mL
oz	gallons	3.785	liters	L
gal	cubic feet	0.028	cubic meters	m^3
ft^3	cubic yards	0.765	cubic meters	m^3
yd^3	NOTE: volumes greater than 1000 L shall be shown in m^3			
		MASS		
oz	ounces	28.35	grams	g
lb	pounds	0.454	kilograms	kg
T	short tons (2000 lb)	0.907	megagrams (or "metric ton")	Mg (or "t")
		TEMPERATURE (exact degrees)		
^oF	Fahrenheit	5 (F-32)/9 (F-32)/1.8	Celsius or	^oC
		ILLUMINATION		
fc	foot-candles	10.76	lux	lx
fl	foot-Lamberts	3.426	candela/m^2	cd/m^2
		FORCE and PRESSURE or STRESS		
lbf	poundforce	4.45	newtons	N
lbf/in^2	poundforce per square inch	6.89	kilopascals	kPa

APPROXIMATE CONVERSIONS FROM SI UNITS

SYMBOL	WHEN YOU KNOW	MULTIPLY BY	TO FIND	SYMBOL
		LENGTH		
mm	millimeters	0.039	inches	in
m	meters	3.28	feet	ft
m	meters	1.09	yards	yd
km	kilometers	0.621	miles	mi
		AREA		
mm^2	square millimeters	0.0016	square inches	in^2
m^2	square meters	10.764	square feet	ft^2
m^2	square meters	1.195	square yards	yd^2
ha	hectares	2.47	acres	ac
km^2	square kilometers	0.386	square miles	mi^2
		VOLUME		
mL	milliliters	0.034	fluid ounces	fl oz
L	liters	0.264	gallons	gal
m^3	cubic meters	35.314	cubic feet	ft^3
m^3	cubic meters	1.307	cubic yards	yd^3
		MASS		
g	grams	0.035	ounces	oz
kg	kilograms	2.202	pounds	lb
Mg (or "t")	megagrams (or "metric ton")	1.103	short tons (2000 lb)	T
		TEMPERATURE (exact degrees)		
^oC	Celsius	1.8C+32	Fahrenheit	^oF
		ILLUMINATION		
lx	lux	0.0929	foot-candles	fc
cd/m^2	candela/m^2	0.2919	foot-Lamberts	fl
		FORCE and PRESSURE or STRESS		
N	newtons	0.225	poundforce	lbf
kPa	kilopascals	0.145	poundforce per square inc h	lbf/in^2

*SI is the symbol for the International System of Units. Appropriate rounding should be made to comply with Section 4 of ASTM E380. (Revised March 2003)

Acknowledgements

The authors thank the Southern Plain Transportation Center (SPTC) for their sponsorship of this study. Also, we would like to thank Mintae Kim, a Ph.D. student, and the following undergraduate students for their assistance in conducting various tests for this study: Garret Hester, Mohan Birbal, Erick Ramirez, Moon Ghimire, and Ferdous Ashrafi. The authors thank Ms. Kim Harris for her administrative support throughout the project.

Tangential Heave Stress Acting on Deep Foundations in Cold Regions

Final Report

May 2019

by

Hoyoung Seo, Ph.D., P.E.
Assistant Professor
Department of Civil, Environmental, and Construction Engineering
Texas Tech University

Liang Li
Graduate Research Assistant
Department of Civil, Environmental, and Construction Engineering
Texas Tech University

William D. Lawson, P.E., Ph.D.
Associate Professor
Department of Civil, Environmental, and Construction Engineering
Texas Tech University

and

Priyantha W. Jayawickrama, Ph.D.
Associate Professor
Department of Civil, Environmental, and Construction Engineering
Texas Tech University

Southern Plains Transportation Center
201 Stephenson Pkwy, Suite 4200
The University of Oklahoma
Norman, OK 73019

TABLE OF CONTENTS

List of Figures

List of Tables

Executive Summary

This project experimentally investigated the effect of frost heave during soil freezing on development of tangential heave stress acting on deep foundations through well-controlled, laboratory-scale frost heave tests on a model pile using a novel testing system developed in this study. A 295-mm-thick soil layer (SIL-CO-SIL 250 silt) was deposited in the soil box, and moisture sensors and thermocouples were embedded in the soil. A model pile, with an outer diameter of 48.3 mm, was designed to minimize disturbances on pile-soil interactions and instrumented with strain gages, thermocouples, and dial gages.

Using the novel testing system, a tangential heave test was performed in an environmental chamber with a temperature gradient of 0.085 °C/mm between the top and bottom of the soil sample. Heave amount of soil surface and pile top movement were monitored using dial gages, while axial strains in pile, moisture variations in soil, and temperature variations in soil were electronically recorded using data acquisition system. Furthermore, images of soil sample during tangential heave test were obtained using high definition digital camera. The maximum heave amounts at the center and corner of the soil surface were 18.0 mm and 14.0 mm, respectively, and the pile top reached a peak upward movement of 0.533 mm. The tangential heave stress measured in this study varied from about 66 kPa to 280 kPa. The tangential heave test system developed in this study was successfully used to investigate various aspects of frost heave process and provided a wealth of information that helps improve understanding of ice-soil-pile interactions focusing on tangential heave stress acting on deep foundations. In particular, given the absence of standard test methods to assess tangential heave stress during soil freezing, the testing system and procedure developed in this study may contribute to establish a test standard for tangential heave testing.

1. INTRODUCTION

1.1 PROBLEM STATEMENT

Foundations in cold regions can be subjected to uplift forces such as a basal heave force and a tangential heave force which are caused by freezing of frost-susceptible soils. In a seasonal frost area, the basal heave force is not a big concern for deep foundations because the foundation base is typically deeper than the frost depth. However, there still exists the tangential heave force (or upward shear force) that acts along the outer surface of the foundation in the frost zone after the adfreeze bond between pile and soil is broken due to frost heave of soil.

Tangential heave stress is defined as the tangential heave force divided by outer surface area of the pile above the frost depth (i.e., the depth of the 0 °C isotherm from the ground surface). Deep foundations in cold regions should be designed in such a way that shaft resistance provided by soils below the frost depth is greater than the tangential heave force induced by heaving soils above the frost depth. When tangential heave force is not properly considered in the design, foundations experience a significant upward movement jeopardizing structural integrity of the superstructure. However, values of tangential heave stress reported in the literature show very large variability. Consequently, pile lengths designed using tangential heave stresses reported in the literature vary greatly. Furthermore, many published studies do not provide details of the test conditions associated with determination of tangential heave stress such as frost depth, water content of soil, and ground temperature. Therefore, proper understanding of the effect of tangential heave stress resulted from the frost action on the foundation elements of transportation infrastructure is extremely important.

1.2 BACKGROUND

Cold regions engineering is a discipline that involves design and construction in the locations that experience very low temperatures. The problem is that the analyses and practices of engineering that are customary in the rest of the world may not be

appropriate in cold regions due to the existence of such low temperatures. In non-cold regions, deep foundations are designed such that they support compressive, tensile, and lateral forces from superstructures. In cold regions, deep foundations are subjected to additional forces arising from frost action of surrounding soils. Tangential heave force and basal heave force are two such examples. The basal heave force refers to the upward force on the bottom of the foundation base. The tangential heave force refers to the upward shear force that acts along the pile due to frost heave after the adfreeze bond between the pile and soil is broken.

When the ground temperature drops below the freezing point, a bond is formed by ice between the foundation material (e.g., steel, concrete, or wood) and the frozen soil, which is the process called adfreezing in *ASTM Standard D 7099-04* (2010). Frost heave of soils in the active layer causes the two objects – i.e., the foundation and the soil – to be separated. The shear stress required to separate an object (i.e., the foundation) from the frozen ground is referred to as the "adfreeze shear strength" in *ASTM Standard D 7099-04* (2010). According to Nidowicz and Shur (1998), the soil in cold regions is initially firmly adfrozen to the surface of foundation in the beginning of winter. As cold temperatures further penetrate into the ground, the frost-susceptible soil surrounding the pile heaves and hence the initial bond between pile and soil – the adfreeze shear strength identified above – is overcome. Soil then slides along the pile for the rest of the frost heave period and the sliding motion of the soil pulls the pile upward. In this report, from this point onward, we will call the upward force and stress as tangential heave force (Q_{hv}) and tangential heave stress (q_{hv}), respectively, the terms used by Kiselev (1973) and Nidowicz and Shur (1998). In design of deep foundations in cold regions, the magnitude of Q_{hv} must be smaller than the shaft resistance (Q_{sL}) of the pile below frost depth (refer to **Figure 1**(a)). The larger the Q_{hv}, the deeper the foundation must be. When the upward forces exceed the shaft resistance below the frost depth, foundations experience significant upward movement (also known as frost jacking) as shown in **Figure 1**(b).

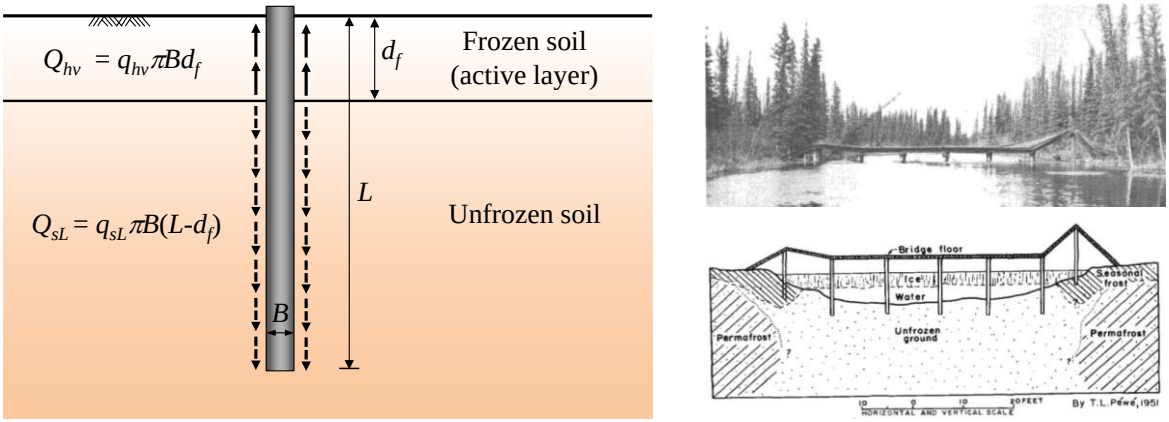

Figure 1. (a) A deep foundation subjected to tangential heave force in cold regions and (b) a photo showing bridge foundations affected by severe tangential heave forces (Pewe and Paige, 1963)

Determination of Q_{hv}, calculated by multiplying the tangential heave stress q_{hv} by the surface area of the foundation element within the frost depth d_f, is one of the most important processes in the design of deep foundations in cold regions (Johnston 1981). However, values of tangential heave stress (q_{hv}) reported in the literature show large variability, with values ranging from 45 kPa to 3,400 kPa. In fact, Nidowicz and Shur (1998) argued that the length of a pile designed using tangential heave stresses suggested in *Technical Manual TM-5-852-4* by U.S. Department of the Army and the Air Force (1983) may be several times greater than one designed according to *Russian Building Code SNiP2.02.04-88* by State Building Committee (1991), depending on loading conditions. One of the reasons why large scatter exists for reported tangential heave stress values appears to be confusion between adfreeze shear strength and tangential heave stress (sometimes called residual adfreeze strength). Despite the experimental observations that the adfreeze shear strength can be more than 10 times greater than the tangential heave stress (Tsytovich 1975), distinctions between the two variables were barely made in previous studies.

Published studies also identify many different methods for measuring the tangential heave stresses due to ground freezing. According to Kim et al. (2015), these methods can be categorized into three different methods based on the main instrumental

apparatus and testing mechanisms: (1) reaction frame and load cell method, (2) strain gage method, and (3) pull-out or jack-in test method. These methods mainly focus on measuring responses at the pile head during frost heaving, but none of these methods measure development of tangential heave stress and shaft resistance along pile length. Furthermore, although interface behavior between a pile and frozen soil is affected by many factors such as soil type, ground temperature, frost depth, water and ice content, material type of pile, and rate and duration of loading, many previous studies provide only limited details of the testing conditions.

A better understanding of soil-pile-water-ice interaction can make a significant contribution to the body of knowledge of cold regions engineering by producing a wealth of information on the development of tangential heave stress. This will help foundation engineers identify and select suitable design values of tangential heave stress for deep foundations in cold regions.

1.3 OBJECTIVES

The goal of this study is to experimentally investigate the effect of frost heave during soil freezing on the development of tangential heave stress acting on deep foundations through well-controlled, laboratory-scale frost heave tests on a model pile. The main objectives of the study include:

(a) Developing laboratory-scale frost heave testing apparatus that can accommodate model piles
(b) Developing instrumented model pile to measure tangential heave force with minimal disturbance
(c) Performing frost heave tests on instrumented model pile and obtaining experimental data including temperature of soil, moisture content of soil, heave amounts of soil and pile, and axial strain on pile
(d) Analyzing measured data to improve understanding of soil-pile-water-ice interactions focusing on tangential heave stress.

2. DEVELOPMENT OF FROST HEAVE TEST SYSTEM

2.1 FROST HEAVE TEST SYSTEM

Frost heave tests have been often performed using a triaxial cell type apparatus connected with cold and hot units (Penner 1986; Akagawa 1988; Xia 2006; Dagli et al. 2018). This type of test setup provides a constant temperature gradient and an excellent visual observation of ice lens formation. However, the small size of triaxial cell is not conducive to performing frost heave test with a model pile installed.

In this study, two different frost heave test apparatuses were developed: (1) a 76-mm-diameter (3-inch-diameter) cylindrical apparatus and (2) a 267-mm-wide (10.5-in-wide) box apparatus. The purpose of 76-mm-diameter cylindrical apparatus was to assess the frost susceptibility of soils using a simple test set up that can be constructed with easily accessible materials. On the other hand, the 267-mm-wide box apparatus was carefully designed to obtain various experimental data such as soil temperature, soil moisture, heave amount, and strain data.

2.1.1 Environmental Chamber

For this project, BEMCO Model FLW-30/65C-340 walk-in environmental chamber was used as a climate controlled room (refer to **Figure 2**). The size of the environment chamber is 2.1 m × 2.1 m × 2.7 m (7 ft x 7 ft x 9 ft), and the temperature can be controlled from + 90 °C (194 °F) to –35 °C (–31 °F). An access port is located on one side of the environmental chamber allowing various cables and hoses to pass through without compromising the insulation. All frost heave tests in this project were performed inside the environmental chamber.

Figure 2. Walk-in environmental chamber used in this study

2.1.2 76-mm-diameter Cylinder Type

The small-scale, cylindrical frost heave test apparatus system mainly consisted of (1) a 76-mm-diameter cylindrical specimen mold, (2) a 152-mm-diameter water bath, and (3) an environmental chamber. As shown in **Figure 3**, the specimen mold was 305 mm in height and its outer surface was wrapped with insulating material. Also, the specimen mold had a 5-mm-diameter hole drilled into the bottom to allow the water uptake. The cylindrical mold was placed in the water bath, and the water level in the water bath was kept at 13 mm above the bottom of the mold. The water temperature was maintained at a target temperature by using a waterproof heating device and a temperature controller. A filter paper was placed on top of the water uptake hole to prevent a test soil from migrating into the water bath while still allowing water inflow.

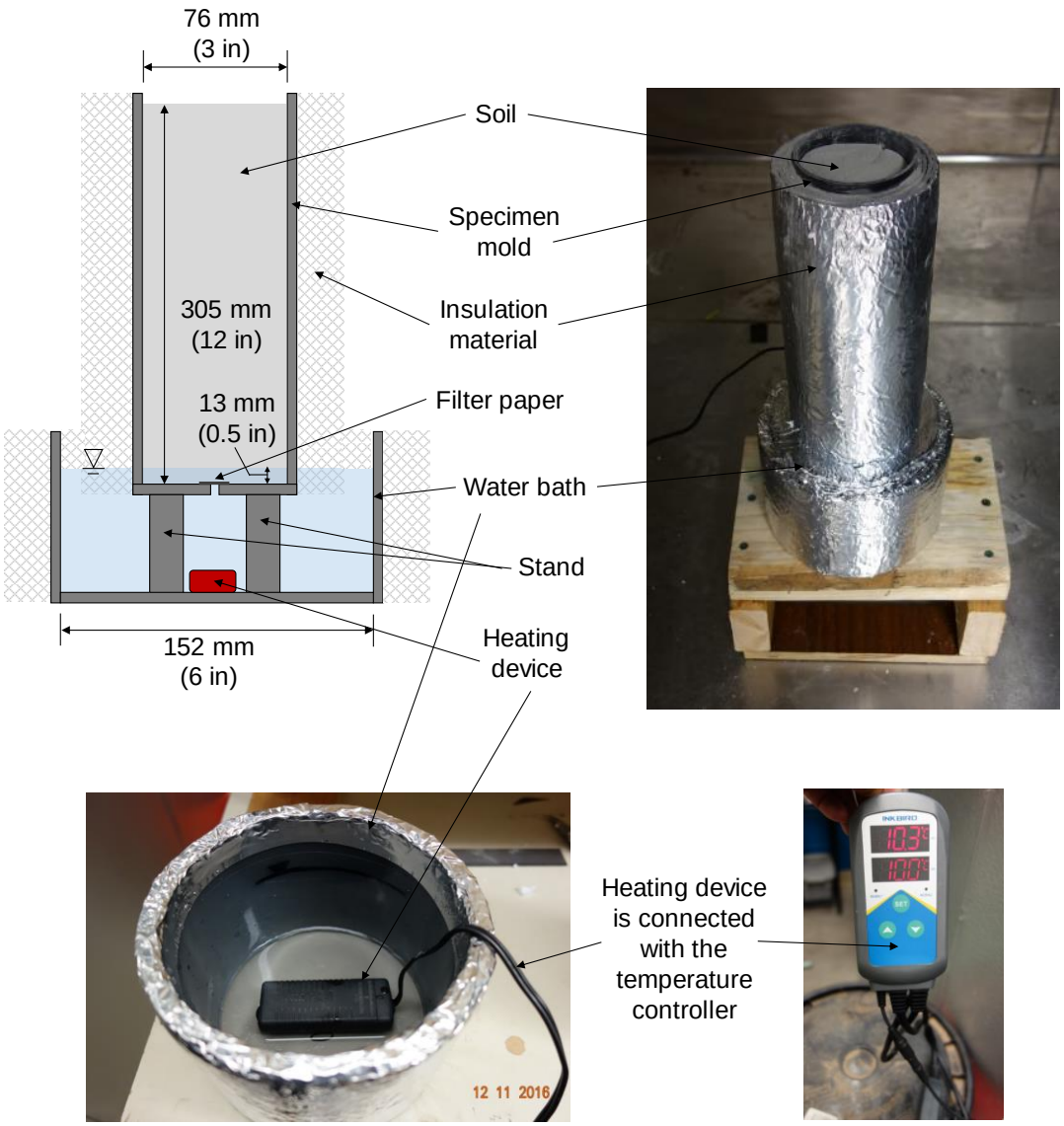

Figure 3. Details of 76-mm-diameter, cylinder-type frost heave test apparatus

The specimen mold and water bath were placed in an environmental chamber and exposed to a cold air during frost heave testing. One of the advantages of the 76-mm-diameter cylinder-type apparatus was that many tests with different temperature gradients were able to perform simultaneously by placing several apparatuses in an environmental chamber and controlling water temperatures in the water bath.

2.1.3 267-mm-wide Box Type

The 267-mm-wide, box-type frost heave test apparatus was carefully designed to accommodate various sensors and a model pile. As shown in **Figure 4**, the box-type frost heave test apparatus consisted of (1) a soil box, (2) constant-head water supply system, and (3) an environmental chamber.

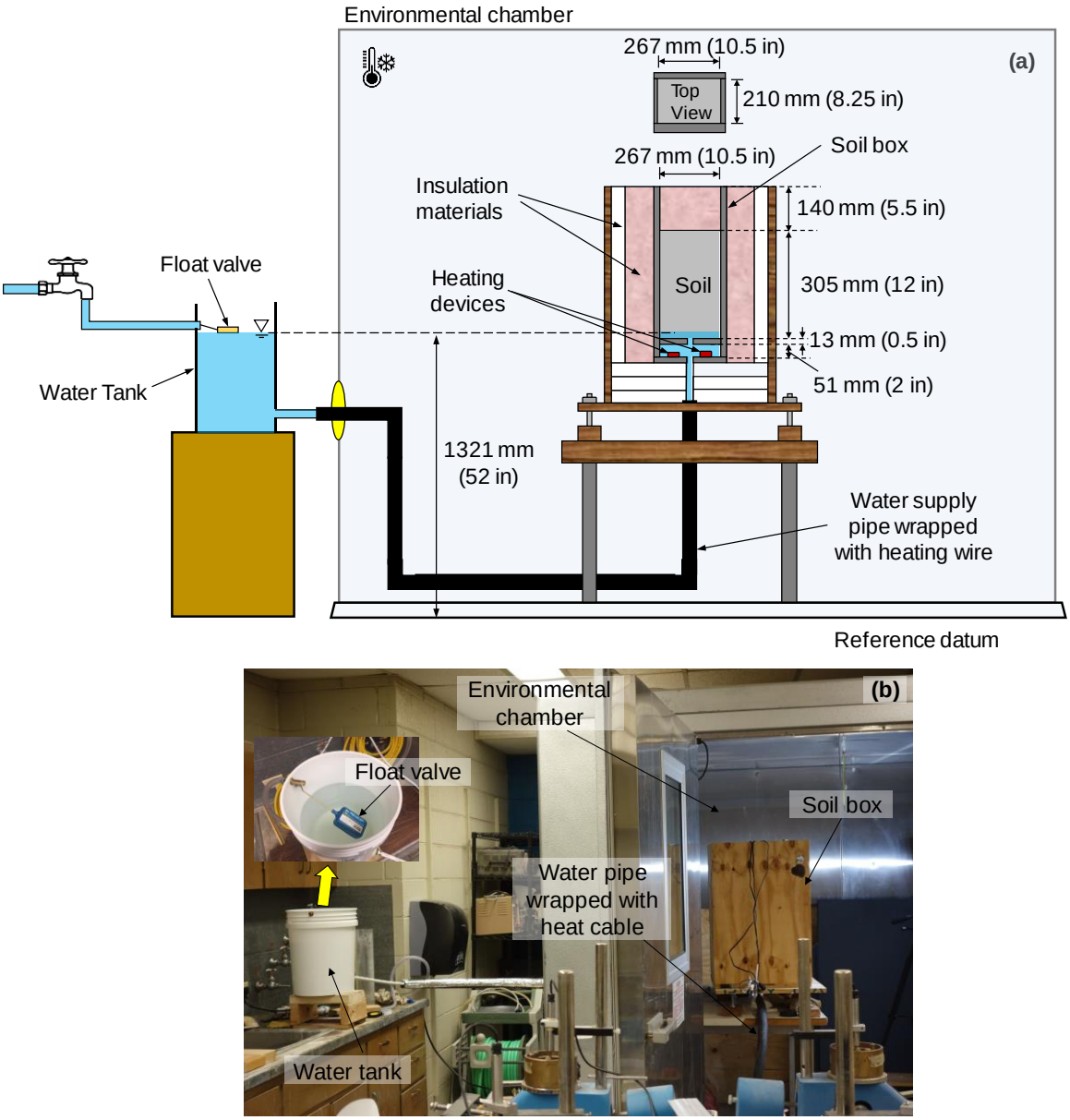

Figure 4. Overview of 267-mm-wide, box-type frost heave test system: (a) a schematic diagram, and (b) a photo

As shown in **Figure 5**(a), the soil box had dimension of 267 mm x 210 mm x 508 mm and was manufactured using Plexiglass plate (thickness of front plate was 18 mm and that for the other plates was 13 mm). The soil box was further separated into top and bottom compartments. Top compartment was 445 mm in height and served as a soil container while the 51-mm-high bottom compartment served as a water bath (refer to **Figure 5**(a)). A 5-mm-diameter hole was drilled into the separation plate to allow water uptake. Heating devices were installed inside of the water bath (bottom compartment) to control the water temperature. The bottom plate of the bottom compartment of the soil box had a 13-mm-diameter hole and was connected to a constant-head water supply system through a water pipe. The soil box was placed inside a wooden box (dimension 521 mm x 445 mm x 699 mm), and the space between the wooden box and soil box were filled with styrofoam boards and fiberglass batts for insulation. Only the top side of the soil box was exposed to the cold air in the environmental chamber to simulate one-dimensional frost penetration process of the field condition. The wooden box had a front door, and the door was open when photos were taken and closed immediately after taking photos to keep the soil box insulated during the testing.

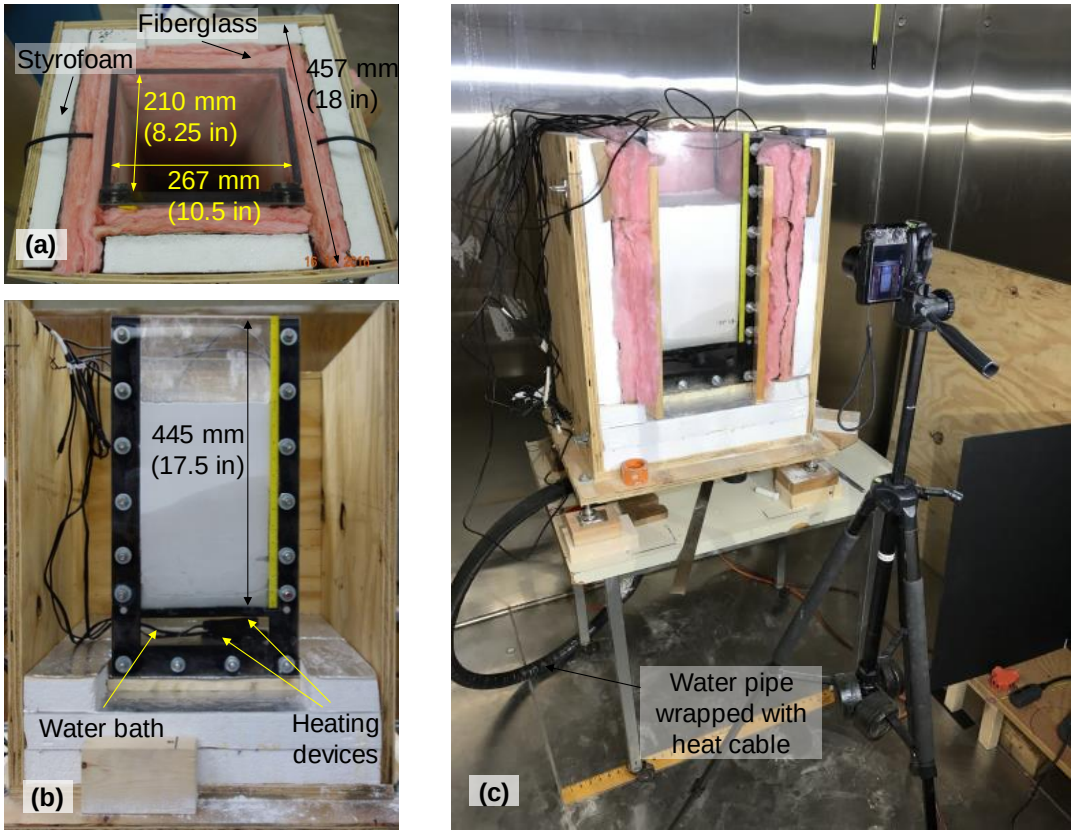

Figure 5. Details of 267-mm-wide soil box: (a) top view, (b) front view, and (c) a view of testing in progress with front door open

The constant-head water supply system was composed of a water tank with a 13 mm-diameter water pipe connected to the bottom of the water bath of the soil box. A water was supplied from a faucet in the laboratory into the water tank, and a float valve was installed in the water tank to maintain constant water level (refer to **Figure 4**). The water pipe was wrapped with a heating cable to prevent from freezing in the environmental chamber during the frost heave testing. The water table in the water tank was kept constant at 1321 mm above the laboratory floor, corresponding to 25 mm above the bottom of the soil sample in the upper compartment of the soil box.

2.2 TEST SOIL

Frost susceptibility refers to the tendency of soil to grow ice lenses and heave during freezing. As the cold front penetrates into soil, pore water freezes in a frost zone. Therefore, about 9% of volume increases when water changes into ice due to the

properties of water and ice. However, the 9% volume change alone does not cause major frost heave problems. Major frost heave is caused by the formation of ice lenses in frozen soil through which water migration occurs from a nearby source.

According to Holtz et al. (2011), three conditions for formation of ice lenses in soils are necessary: 1) temperature below freezing, 2) source of water close enough to supply capillary water to the frost line, and 3) frost-susceptible soil type and grain (or pore) size distribution. The American Concrete Pavement Association (ACPA, 2008) classified the degree of the frost susceptibility based on two hydraulic properties of soils: 1) capillarity and 2) permeability. Soils with very small voids such as highly plastic clays have high capillarity but the volume of water available to form ice lenses is limited because of low permeability and, therefore, highly-plastic clays are less susceptible to frost action than silty soils which are more permeable. On the other hand, clean sands and gravels have high permeability due to their large pore sizes but because of low capillarity, water cannot migrate to the frost line. Therefore, clean sands and gravels are less susceptible to frost action than silty soils which have higher capillarity. This concept is illustrated in **Figure 6**.

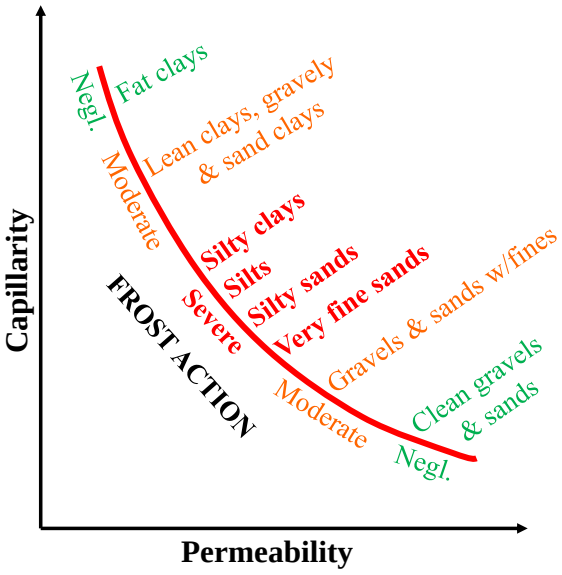

Figure 6. Frost susceptibility based on two hydraulic properties of soils (modified after ACPA 2008)

A common guideline to assess frost susceptibility was initially developed by Casagrande (1932). The Casagrande guideline relates frost susceptibility of soils to the percentage of fine fraction less than 0.02 mm. U.S. Department of Defense (USDOD, 2001) extended the Casagrande guideline and classified the frost susceptibility of soils as shown in **Table 1**. **Table 1** shows that the frost susceptibility of clean sands (SP and SW) and clean gravels (GP and GW) is classified as negligible or very low. On the other hand, silty sands, silts, and clayey silts are classified as highly susceptible to frost actions. This classification is overall in good agreement with **Figure 6** by ACPA (2008).

Table 1. Frost Susceptibility Classification (USDOD, 2001)

Frost Group	Frost Susceptibility Classification	Soil Type	Percentage Finer than 0.02 mm by Weight	Typical Soil Types Under Unified Soil Classification System (USCS)
NFS[(a)]	Negligible	Gravels	0-1.5	GW, GP
NFS[(a)]	Negligible	Crushed Stone	0-1.5	GW, GP
NFS[(a)]	Negligible	Crushed Rock	0-1.5	GW, GP
NFS[(a)]	Negligible	Sands	0-3	SW, SP
PFS[(b)]	Negligible to Very Low	Gravel	1.5-3	GW, GP
PFS[(b)]	Negligible to Very Low	Crushed Stone	1.5-3	GW, GP
PFS[(b)]	Negligible to Very Low	Crushed Rock	1.5-3	GW, GP
PFS[(b)]	Negligible to Very Low	Sands	3-10	SW, SP
S1	Very Low	Gravelly Soils	3-6	GW, GP, GW-GM, GP-GM
S2	Very Low	Sandy Soils	3-6	SW, SP, SW-SM, SP-SM
F1	Low	Gravelly Soils	6-10	GM, GW-GM, GP-GM
F2	Medium	Gravelly Soils	10-20	GM, GW-GM, GP-GM
F2	Medium	Sands	6-15	SM, SW-SM, SP-SM
F3	High	Gravelly Soils	> 20	GM, GC
F3	High	Sands, except very fine silty sands	> 15	SM, SC
F3	High	Clays, PI > 12	--	CL, CH
F4	Very High	Silts	--	ML, MH
F4	Very High	Very fine silty sands	> 15	SM
F4	Very High	Clays, PI <12	--	CL, CL-ML
F4	Very High	Varved clays and other fine grained, banded sediments	--	CL and ML; CL, ML, and SM; CL, CH, and ML; CL, CH, ML, and SM

Notes:

(a) Non-frost susceptible

(b) Possibly frost susceptible, but requires laboratory test to determine frost susceptibility.

(c) USDOD (2001) considers soils categorized as NFS, PFS, S1, and S2 to be suitable as base and subbase course material for pavement design. Soils categorized as F1, F2, F3, and F4 are considered to be unsuitable as base or subbase material.

The classification system is in order of increasing frost susceptibility and loss of subgrade strength upon thawing.

In this study, five different types of soils that are commercially available have been tested to assess frost susceptibility and to identify the most suitable soil for this project: 1) F-55 sand, 2) Ruby Mountain Stone Flour, 3) Microfine Basalt, 4) Glacier Stone Dust,

and 5) SIL-CO-SIL-250 Silica Powder. Sieve analysis and hydrometer tests were performed to determine the gradation of the soils. Particle size distribution curves of these soils are presented in **Figure 7**. Atterberg limit tests were also performed to determine the plasticity of the test soils. **Table 2** summarizes properties of the test soils.

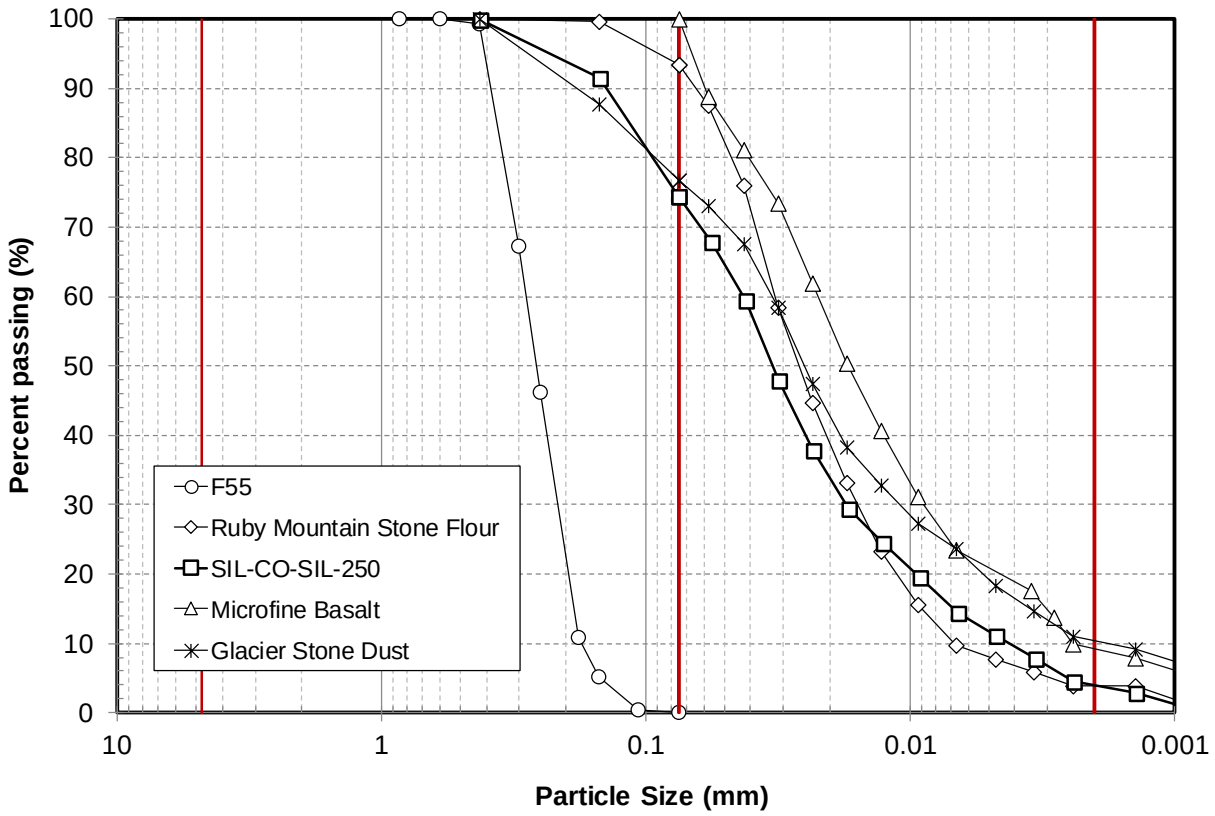

Figure 7. Particle size distribution curves of test soils

Table 2. Properties of test soils

Commercial Name	Soil Type	USCS Group Symbol	D_{50} (mm)	PI	Percent Passing #200	Percent finer than 0.02 mm	Vendor
F-55 sand	Fine sand	SP	0.26	NP	0	0	US Silica
Ruby Mountain Stone Flour	Silt	ML	0.027	NP	93	38	Rock Dust Local LLC
Microfine Basalt	Silt	ML	0.017	2	100	55	Rock Dust Local LLC
Glacier Stone Dust	Silt	ML	0.025	NP	77	42	Nature's Footprint
SIL-CO-SIL-250 Silica Power	Silt	ML	0.033	NP	75	33	US Silica

Note: PI = plasticity index; NP = non-plastic

2.3 TEST PROCEDURE AND RESULTS

2.3.1 Frost heave tests using 76-mm-diameter cylinder-type apparatus

Because the main purpose of the 76-mm-diameter cylinder test was to assess frost susceptibility of different soil types and to identify optimal testing conditions, several tests were performed in the environmental chamber simultaneously. Testing procedures were as follows:

(1) Prepare a soil specimen in the cylindrical mold to a height of 305 mm.

(2) Put the cylindrical mold into a water bath.

(3) Pour the water into a water bath until the water level reaches 25 mm higher than the elevation of the bottom of the soil sample.

(4) Wait until the soil becomes fully saturated due to capillary rise (typically, it took about 24 hours to achieve full saturation).

(5) Put the mold and water bath in an environmental chamber.

(6) Set the target water temperature using the temperature controller and heating device.

(7) Turn on the environmental chamber and set the air temperature.

(8) Run the tests for at least one week. If no change in sample height is observed, stop the tests.

(9) Extrude the soil sample out of the mold and observe the presence of the ice lens.

During the frost heave testing, water was manually supplied into the water bath to maintain the target water level. It was observed that the water level was decreasing fast in the beginning of the test but showed minimal change after certain durations of the testing.

As the first batch of samples, two types of soils were purchased and tested: F55 sand and Ruby Mountain Stone Flour. The research team took the images of scanning electron microscope (SEM) of these soil samples and they are given in **Figure 8**. Air temperature of the environmental chamber was set to –10 °C and the water temperatures in the baths varied from 10 °C to 20 °C, corresponding to a temperature gradient of 0.066 °C/mm to 0.1°C/mm, respectively, between the top and bottom of the soil sample.

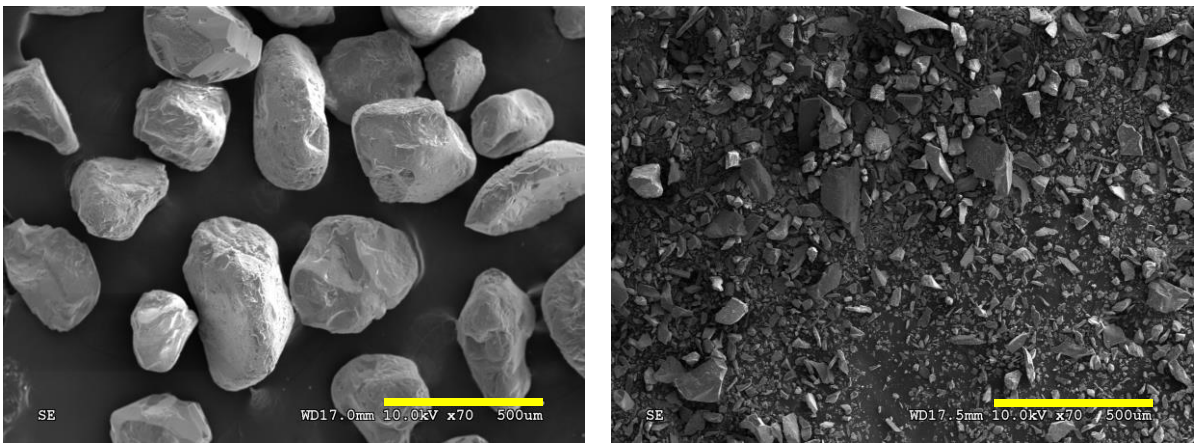

(a) (b)

Figure 8. Scanning electron microscope (SEM) images of first batch of testing soils: (a) F-55 sand magnified by 70x (length of yellow bar = 0.5 mm) and (b) Ruby Mountain Stone Flour magnified by 70x (length of yellow bar = 0.5 mm)

After completion of tests, samples were extruded from the cylindrical mold and cut vertically. F55 sand did not show any ice lens regardless of temperature gradients, but many ice lenses were observed in Ruby Mountain Stone Flour sample from both temperature gradients with the thickest ice lens being 8 mm from temperature gradient of 0.1°C/mm, as shown in **Figure 9**.

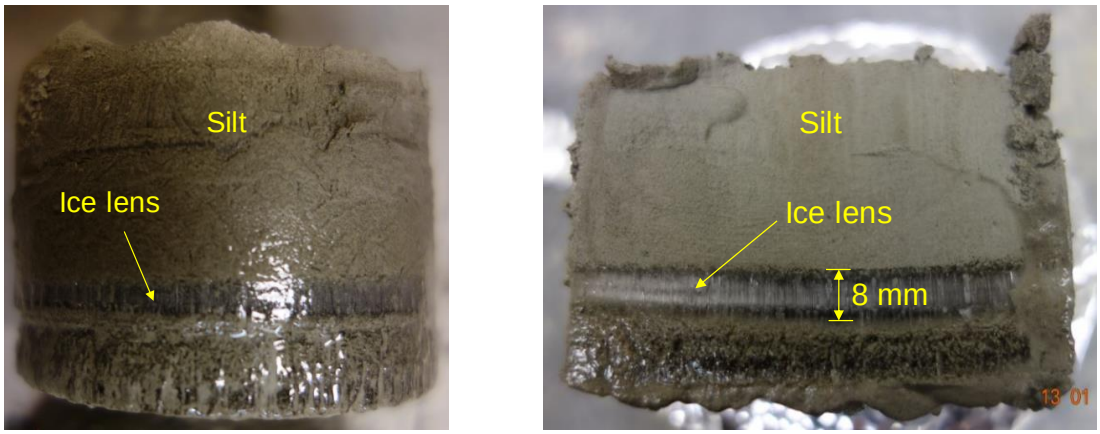

(a) (b)

Figure 9. Photos of ice lens formed in Ruby Mountain Stone Flour: (a) top portion of the extruded sample and (b) vertical cut of the extruded sample (testing conditions: air temperature of environmental chamber = –10 °C; water temperature in water bath = 20 °C; temperature gradient = 0.1°C/mm; testing duration = 17 days)

Since Ruby Mountain Stone Flour was identified as a highly frost susceptible soil from the 76-mm-diameter cylinder test, additional tests were performed using the 267-mm-wide box-type apparatus to confirm its frost susceptibility in a larger scale. Ice lenses were observed in the 267-mm-wide box-type apparatus as well. After confirming its high frost susceptibility in the 267-mm-wide box-type apparatus, the research team contacted the supplier to purchase Ruby Mountain Stone Flour in large quantities for further testing. However, the supplier informed the research team that Ruby Mountain Stone Flour was out of stock for immediate sale and would not be available within the project period because the source rock had to be mined and grinded. The research team then purchased the second batch of testing soils from other sources that are similar to Ruby Mountain Stone Flour in terms of gradation. The second batch of soil samples were Microfine Basalt, Glacier Stone Dust, and SIL-CO-SIL-250.

Frost heave tests using the 76-mm-diameter cylinder apparatus were performed on the three soils from the second batch. A temperature gradient between the top and bottom

of the soil sample ranged between 0.066 °C/mm and 0.1°C/mm. Among the three samples, ice lenses were observed in Glacier Stone Dust and SIL-CO-SIL-250 but no ice lens was observed in Microfine Basalt. The research team selected SIL-CO-SIL-250 as a final test soil because Glacier Stone Dust included many impurities such as plant roots. SEM images of SIL-CO-SIL-250 are given in **Figure 10**. A summary of frost heave test results from the first and second batches of the soil samples using the 76-mm-diameter cylindrical apparatus are presented in **Table 3**.

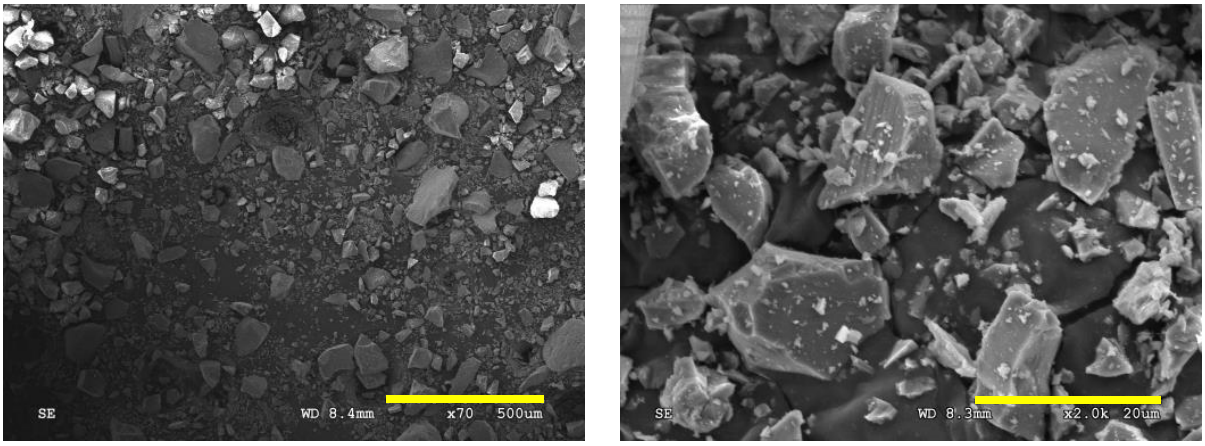

(a) (b)

Figure 10. Scanning electron microscope (SEM) images of SIL-CO-SIL-250: (a) magnified by 70x (length of yellow bar = 0.5 mm) and (b) magnified by 2000x (length of yellow bar = 0.02 mm)

Table 3. A summary of frost heave test results performed on first and second batches of soil samples using 76-mm-diameter cylinder-type apparatus

Batch number	Commercial Name	Soil Type	USCS Group Symbol	Air temp. (°C)	Water temp. (°C)	Temp. gradient (°C/mm)	Testing duration (days)	Thickest ice lens thickness (mm)
1	F-55 sand	Fine sand	SP	–10	10	0.066	13	Not observed
1	Ruby Mountain Stone Flour	Silt	ML	–10	10	0.066	10	2.5
				–10	20	0.1	17	8
2	Microfine Basalt	Silt	ML	–10	20	0.1	21	Not observed
2	Glacier Stone Dust	Silt	ML	–10	10	0.066	21	1.5
2	**SIL-CO-SIL-250 Silica Powder**	**Silt**	**ML**	**–10**	**15**	**0.082**	**30**	**2.5**

2.3.2 Frost heave tests using 267-mm-wide box-type apparatus

As mentioned previously, the main purpose of the 267-mm-wide box-type apparatus was to accommodate various sensors and a model pile. Before performing tangential heave tests with a model pile, a frost heave test was performed using SIL-CO-SIL-250 without a model pile. Three moisture sensors (model name: Decagon 5TM) with built-in thermistors were embedded in the testing soil at a distance of 51 mm (2 in) from one another with the bottommost sensor located at 127 mm above the bottom of the soil sample. To measure the amounts of frost heave, two dial gages were placed at the center and corner of the soil surface. Decagon Em50 Data Logger was used to collect the moisture and temperature measurements. **Figure 11** shows instrumentation details of the 267-mm-wide soil box.

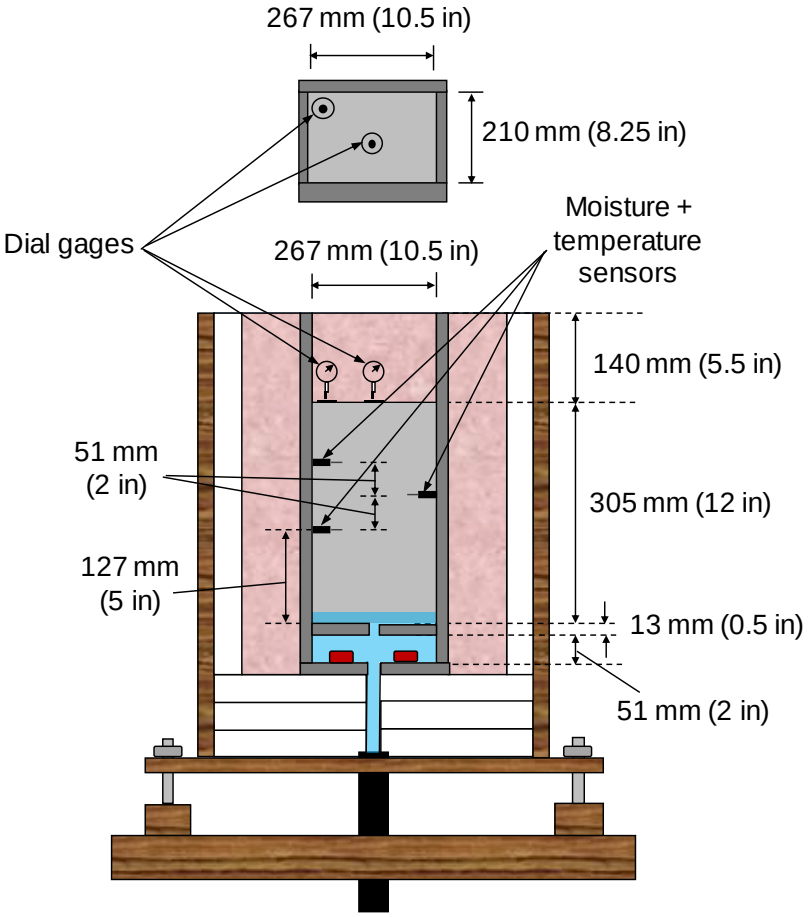

Figure 11. Instrumentation details of 267-mm-wide box-type apparatus for frost heave testing

Testing procedures were as follows:

(1) Start depositing test soil in the soil box (**Figure 12**(a)).

(2) When reaching the target elevation of the moisture sensor, level the soil surface and place the moisture sensor (**Figure 12**(b)).

(3) Add more soils until reaching the target elevation of the next moisture sensor and place the moisture sensor.

(4) Repeat this procedure to install all three moisture sensors.

(5) Add more soils until reaching a total height of 305 mm of soil sample (**Figure 12**(c)).

(6) Place the 267-mm-wide box-type apparatus into the environmental chamber.

(7) Connect the water bath to constant-head water tank and saturate the soil sample through capillary rise (**Figure 12**(d)).

(8) After saturation process is completed, insulate the soil box with fiberglass batts and styrofoam boards.

(9) Connect the moisture sensors with the data logger and place dial gages on the soil surface (**Figure 12**(e)).

(10) Close the front wood door of the soil box (**Figure 12**(f)).

(11) Set the target water temperature of the water bath using the temperature controller and heating device.

(12) Turn on the environmental chamber, set the air temperature, and start running the test.

(13) Take dial gage readings regularly and take photos of soil sample by opening the front door; data from moisture sensors were recorded electronically using a data logger.

(14) After a certain duration, stop the test.

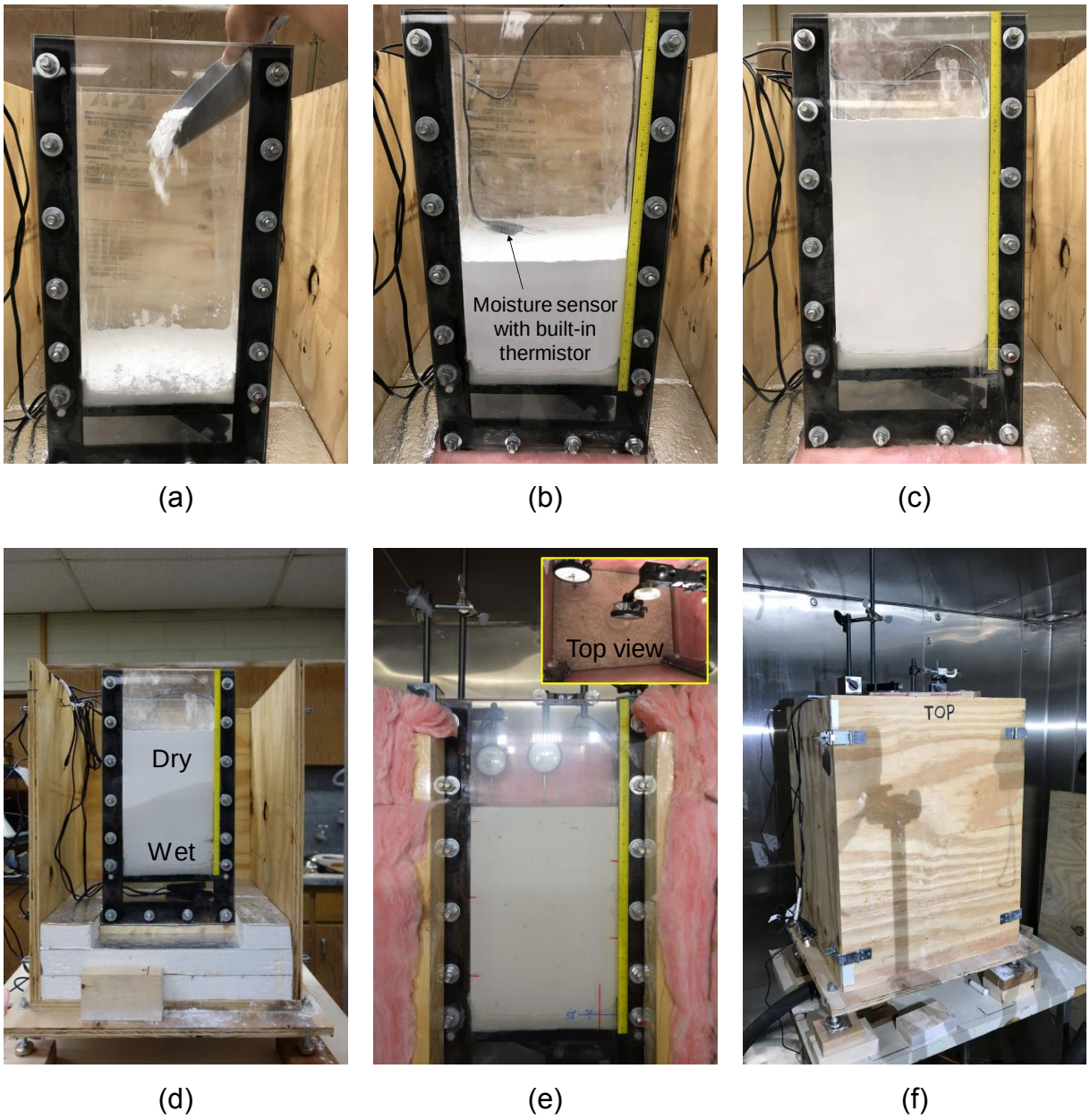

Figure 12. Photos showing test procedures: (a) deposition of testing soil in a soil box, (b) installation of moisture sensor, (c) completion of soil deposition, (d) saturation of soil sample, (e) installation of dial gages, and (f) testing in progress

After completion of saturation, the height of soil sample at the start of frost heave testing was 300 mm. Air temperature of the environmental chamber was set to –10 °C and the water temperatures in the bath set to be 10 °C, corresponding to a temperature gradient of 0.066°C/mm between the top and bottom of the soil sample.

Frost heave test began on September 6, 2017 and ended on November 10, 2017 for a total duration of 65 days (1560 hrs). Amounts of frost heave measured at the center and corner of the soil surface are presented in **Figure 13**. Greater amounts of frost heave was observed at the center than at the edge throughout the testing. The soil sample started heaving very quickly initially and the heave rate gradually decreased with increasing time. After about 400 hours, no frost heave was observed. The frost heave rates at the center of the soil surface about every 50 hour until reaching until 400 hours are presented in **Table 4**.

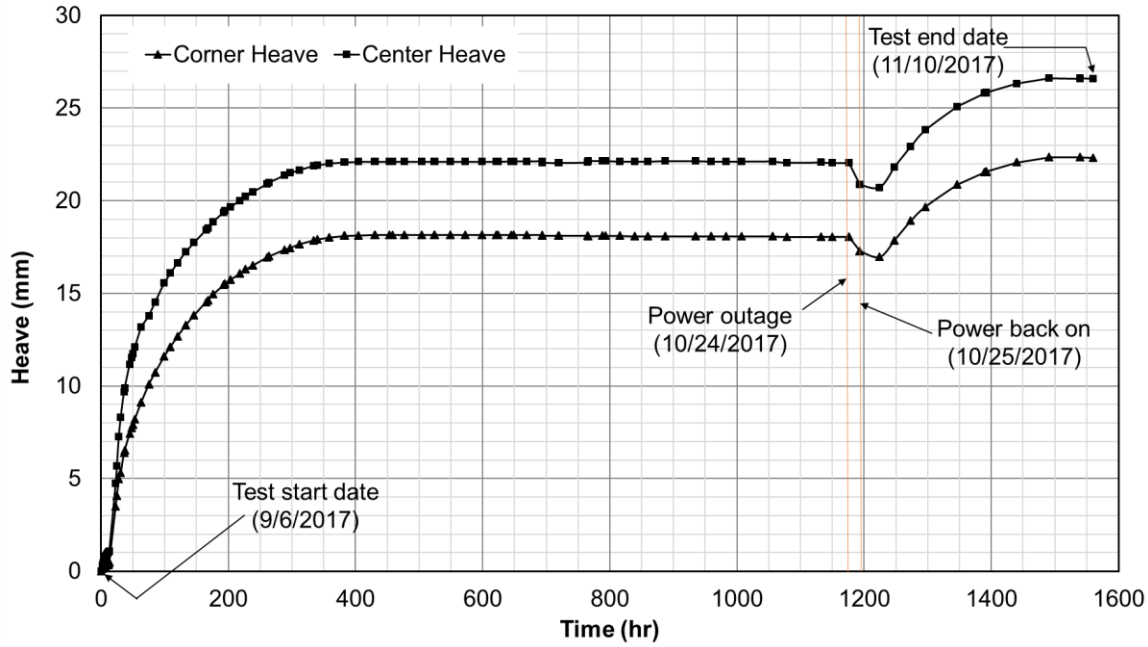

Figure 13. Amounts of frost heave measured at the center and corner of the soil surface versus time (testing conditions: air temperature of environmental chamber = –10 °C; water temperature in water bath = 10 °C; temperature gradient = 0.066°C/mm; test soil = SIL-CO-SIL-250)

Table 4. Frost heave rates at the center of soil surface about every 50 hour until reaching 400 hours

Time (hour)	Heave amount at center (mm)	Heave rate (mm/hr)	Heave rate (mm/day)
0	0	-	-
50	11.735	0.235	5.63
99	15.558	0.078	1.87
146	17.742	0.046	1.12
203	19.660	0.034	0.81
239	20.485	0.023	0.55
297	21.501	0.018	0.42
359	22.022	0.008	0.20
405	22.111	0.006	0.14

While running the test, there was an unexpected campus-wide power outage on October 24, 2017 (48 days after the test began) and the power was restored on next day (October 25, 2017). The heave amount measured at the center of soil surface right before the power outage (elapsed time = 1176 hrs) was 22.047 mm. During the power outage, the surface of the soil settled because the ice melted. After the melting, the soil started heaving again and reached a total frost heave of 26.619 mm at the center of the soil surface at the end of the testing (elapsed time = 1560 hrs).

Figure 14 shows images of soil sample taken through the transparent front wall of the soil box at various elapsed times. The sign of ice lens first appeared after 240 hours and the actual first ice lens was observed at about 168 mm above the bottom of the soil sample after about 540 hours. Typically, a newer ice lens is formed at a deeper depth than the older ice lenses because cold front penetrates deeper with increasing time until a thermal balance is achieved. However, from this test, newer ice lenses were formed at shallower depths than the previous, older ice lenses. For example, at the elapsed time of 816,1008, 1176 hours, the locations of ice lenses from the bottom of the soil sample were 176 mm, 194 mm and 202 mm, respectively. Furthermore, the old ice lenses were melted away when the new ice lens was formed (refer to photos taken at 816, 1008, and 1176 hrs from **Figure 14**). This behavior was observed until the power outage happened and the power was restored (refer to photo taken at 1200 hr).

Then, at 1248 hours (about 48 hours after the power restoration), a new ice lens was formed at about 222 mm above the bottom of the soil sample. After that, the newer ice lenses started forming below the old ice lens (refer to photos taken at 1296 and 1560 hrs). This appears to be due to the change in thermal balance condition during the test and is explained in a later section.

Figure 14. Images of soil sample taken at various elapsed times (testing conditions: air temperature of environmental chamber = –10 °C; water temperature in water bath = 10 °C; temperature gradient = 0.066°C/mm; test soil = SIL-CO-SIL-250)

Figure 15 shows variations of soil temperature, measured from the built-in thermistor of the moisture sensor, versus elapsed time. The three moisture sensors were located 127, 178, and 229 mm above the bottom of soil sample. In the beginning of the test, all three sensors in the soil showed an initial temperature of about 17.5 °C, which was the temperature of the faucet water. After the test began, soil temperatures dropped very quickly and reached equilibrium conditions at 230 hours. The bottommost sensor and another sensor right above it showed temperature values greater than 0°C at 230 hours, but the topmost sensor showed a temperature less than 0°C, indicating the presence of frozen soil. This condition was maintained until about 360 hours, but then the temperatures started gradually increasing thereafter until the power outage happened. After the power was restored, all three sensors showed temperature above 0°C and reached equilibrium conditions from about 1250 hours until the end of the test.

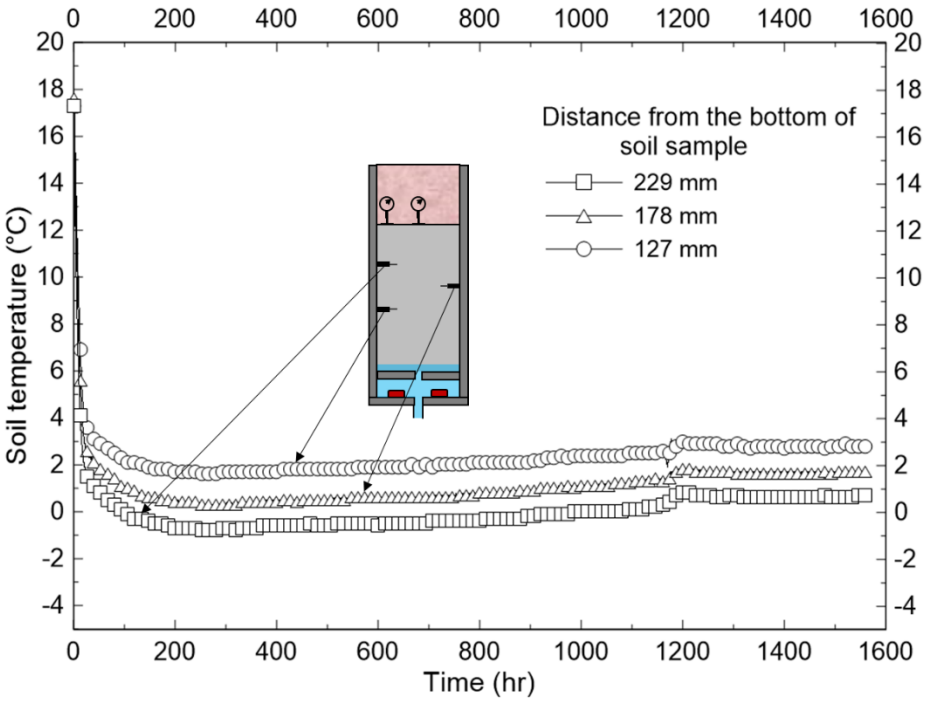

Figure 15. Temperature at various depths of soil sample versus time (testing conditions: air temperature of environmental chamber = –10 °C; water temperature in water bath = 10 °C; temperature gradient = 0.066°C/mm; test soil = SIL-CO-SIL-250)

Figure 16 shows soil temperature versus the distance from the bottom of soil sample. As mentioned previously, a thermal balance was achieved at about 230 hours after the

test began and maintained constant temperatures until reaching elapsed time of 360 hours (**Figure 16**(a)). Until reaching 360 hours, a frost depth (i.e., a depth where the soil temperature is 0 °C) became deeper with increasing time and a linear interpolation suggested that the frost depth was located at about 200 mm above the bottom of soil sample at 360 hours. However, after 360 hours, soil temperatures started increasing and frost penetration depth became shallower, locating at about 235 mm above the bottom of soil sample at 1560 hour. Such increase in temperature (and, therefore, decrease in the frost depth) from about 360 hours to 1200 hours explains why the newer ice lenses were formed above the older ice lenses.

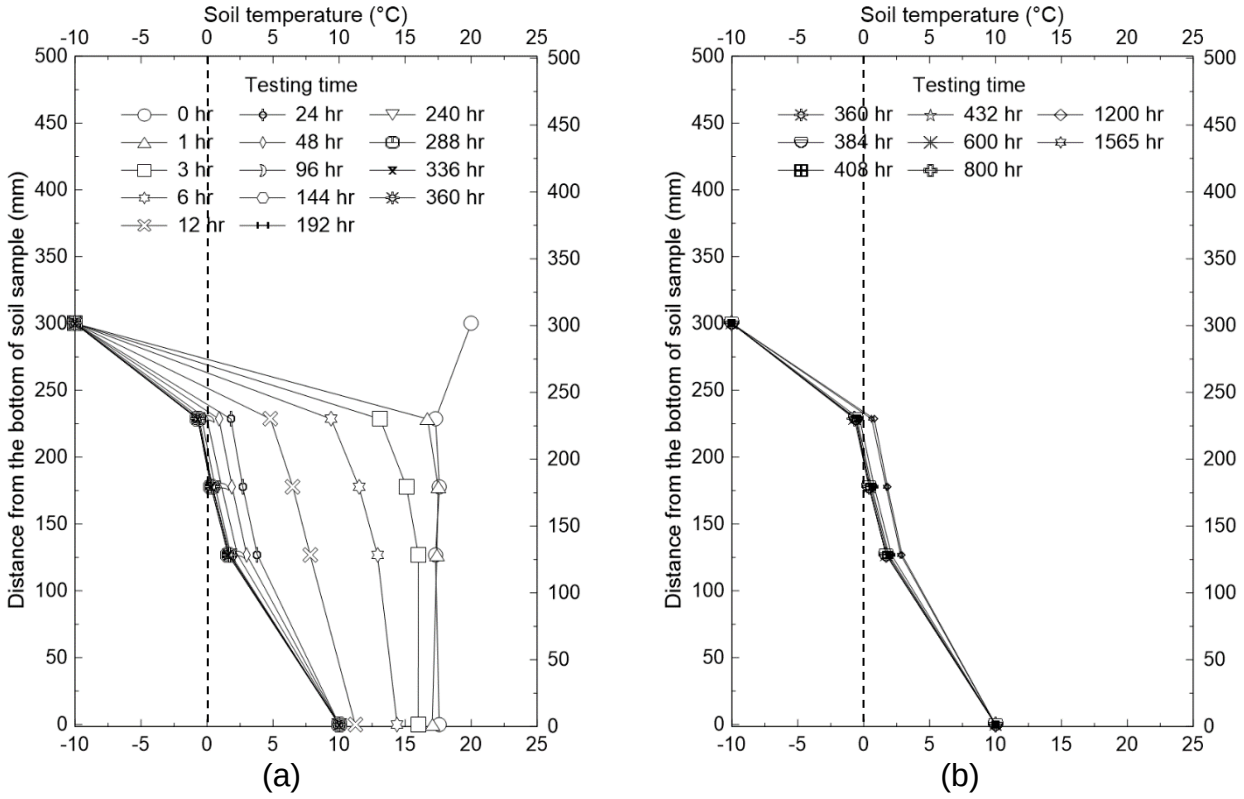

Figure 16. Soil temperature versus distance from the bottom of the soil sample at various elapsed times: (a) 0 – 360 hr and (b) 360 – 1565 hour (testing conditions: air temperature of environmental chamber = –10 °C; water temperature in water bath = 10 °C; temperature gradient = 0.066°C/mm; test soil = SIL-CO-SIL-250)

The reason why the soil temperature started increasing from about 360 hours was presently unknown but probably the moisture sensors might have generated small amount of heat due to prolonged operations with frequent measurements (in this frost

heave test, the data logger was set to measure moisture and temperature values every 1 minute).

Figure 17 shows variations of volumetric water content measured from the three moisture sensors versus elapsed time, and **Figure 18** shows volumetric water contents versus depth at various elapsed times. In the beginning of the test, all three sensors showed initial volumetric water content of about 31%. The volumetric water content from the bottommost sensor did not show any significant change throughout the testing; the moisture sensor right above the bottommost sensor showed similar behavior. However, the volumetric water content measured from the topmost sensor showed a substantial decrease from 75 hours after the test begun due to the cold air coming from the environmental chamber and reached a value as low as about 7% at about 275 hours, indicating that soil became drier (change of the soil color near the ground surface in **Figure 14** clearly showed this behavior). The volumetric water content from the topmost sensor then started gradually increasing and, from about 900 hours, it showed drastic increase. This is because ice in the frozen soil started melting away at the location of the topmost sensor from about 900 hours, and **Figure 15** clearly suggests that soil temperature became greater than 0 °C around 900 hours.

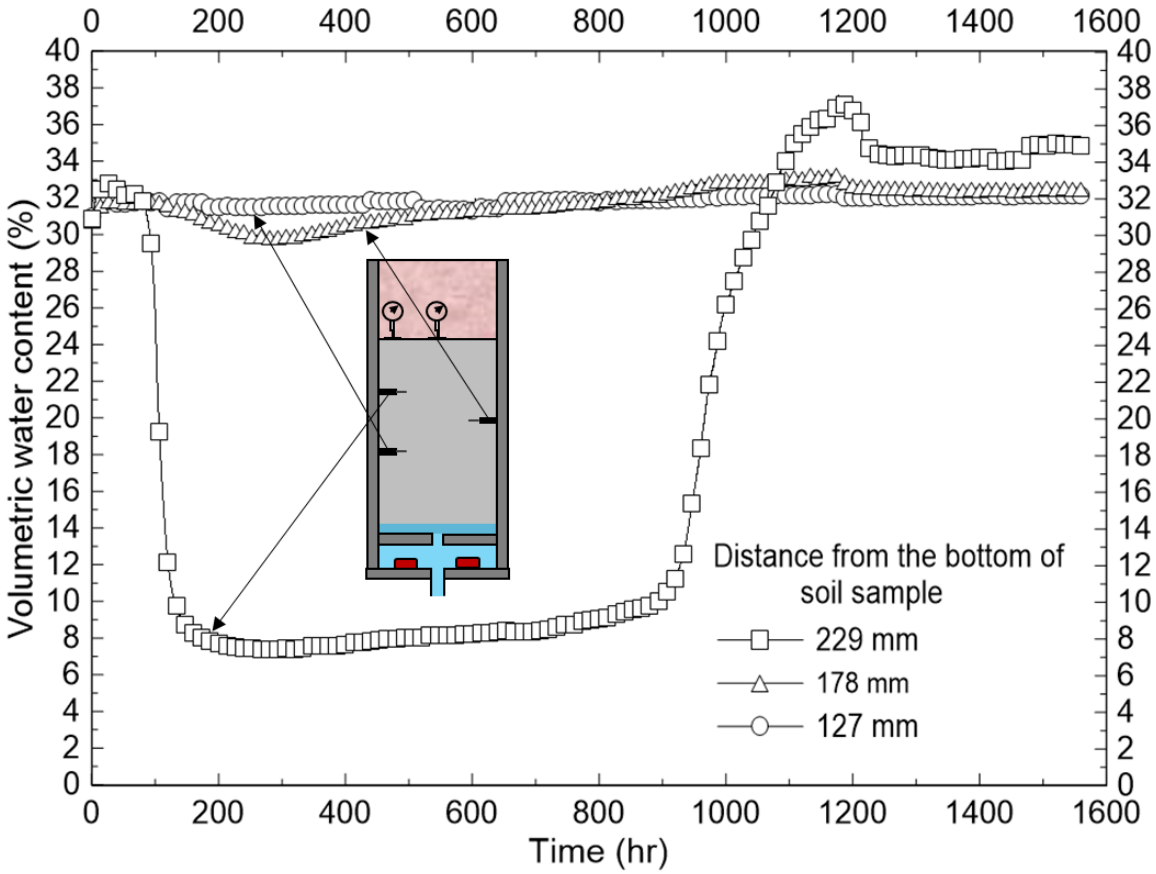

Figure 17. Volumetric water content at various depths of soil sample versus time (testing conditions: air temperature of environmental chamber = –10 °C; water temperature in water bath = 10 °C; temperature gradient = 0.066°C/mm; test soil = SIL-CO-SIL-250)

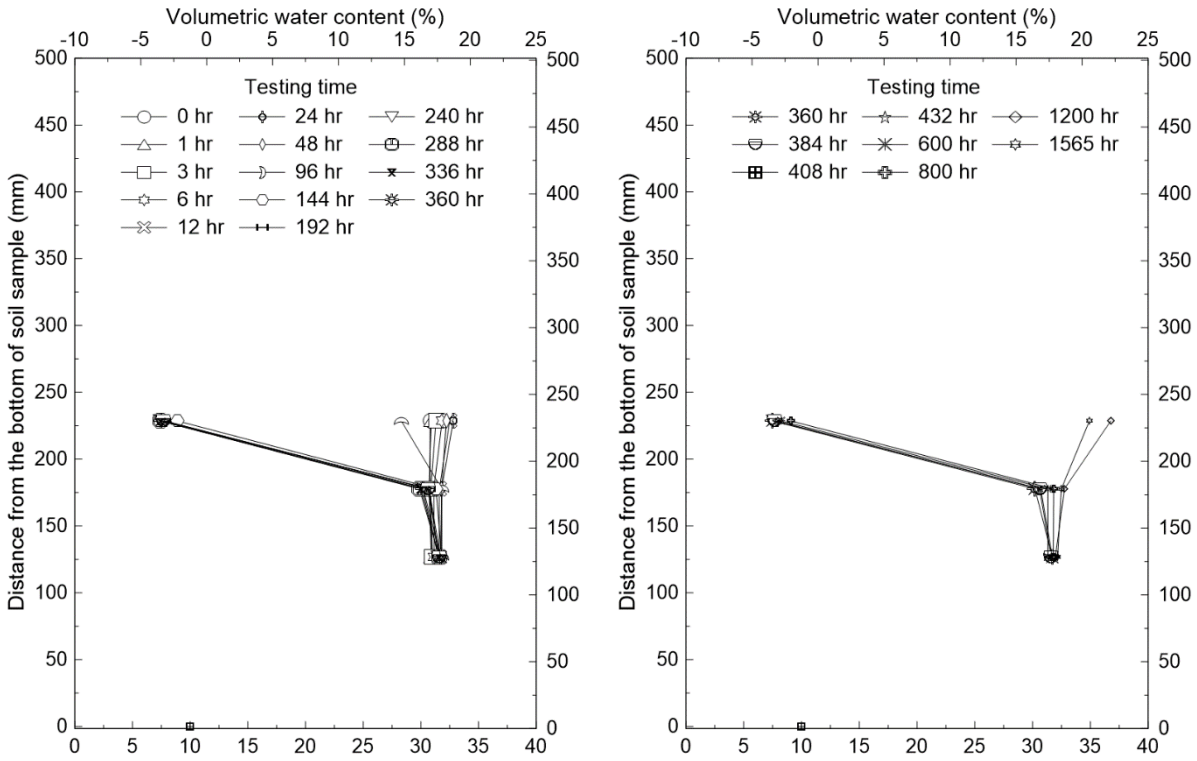

Figure 18. Volumetric water content versus distance from the bottom of the soil sample at various elapsed times (testing conditions: air temperature of environmental chamber = –10 °C; water temperature in water bath = 10 °C; temperature gradient = 0.066°C/mm; test soil = SIL-CO-SIL-250)

2.4 SUMMARY

Two different frost heave test apparatuses were developed: (1) a 76-mm-diameter cylinder-type apparatus and (2) a 267-mm-wide box-type apparatus. The 76-mm-diameter cylindrical apparatus was easy to build and enabled the research team to assess frost-susceptibility of various soil types simultaneously. The 267-mm-wide box apparatus not only successfully simulated frost heave process in a larger scale but also provided various experimental data such as soil temperature, soil moisture, heave amount, and images of ice lens formation process during frost heave testing.

3. TANGENTIAL HEAVE TESTING

This chapter documents the research team's experimental study to investigate the tangential heave force acting on deep foundation during soil freezing. The 267-mm-wide box-type frost heave apparatus was used to simulate the soil freezing process, and a model pile instrumented with strain gages and thermocouples was installed in the test soil. Data were recorded electronically using a data acquisition system, and high-definition images were taken using a digital camera during the testing.

3.1 REVIEW OF TANGENTIAL HEAVE TEST METHODS

Kim et al. (2015) classified the methods for measuring the upward forces (or tangential heave forces) acting on piles due to ground freezing into three categories based on the main instrumental apparatus and testing mechanisms: (1) reaction frame and load cell method (RFLCM), (2) strain gage method (SGM), and (3) pull-out or jack-in test method (POJIM).

The RFLCM utilizes a reaction system and a load cell to measure the force acting on foundations caused by ground freezing. A reaction frame is embedded or anchored to a fixed layer such as bedrock or permafrost, and a load cell is placed at the head of the test pile (refer to **Figure 19**(a)). The upward force acting on the test pile due to ground freezing is measured by the load cell and then divided by the outer surface area of the pile within the frost depth to obtain the stress value.

The SGM utilizes the shaft resistance of the soil below the active layer as a reaction force (refer to **Figure 19**(b)). The strain gages measure axial strains acting on the piles within the active layer, and the strain values are converted to forces using pile stiffness. Then, the upward stress values are computed by dividing the difference in force values from two adjacent strain gages by outer surface area of the pile between the two strain gages.

The POJIM measures frictional resistance between pile and soil by jacking in or pulling out the test pile installed in frozen soil (see **Figure 19**(c)). It should be noted that this

method does not directly measure the upward force exerted by soil due to frost heave; rather, it determines the force-displacement behavior of the interface between pile and frozen soil before and after the adfreeze bond is broken. However, by sufficiently displacing the test pile through the frozen soil, it is assumed that the pull-out or jack-in force at large pile displacements would be very similar to the tangential heave force due to soil heaving after the adfreeze bond is broken. Tangential heave stress is then obtained by dividing the pull-out or jack-in force by the outer surface area of pile that is in contact with frozen soil.

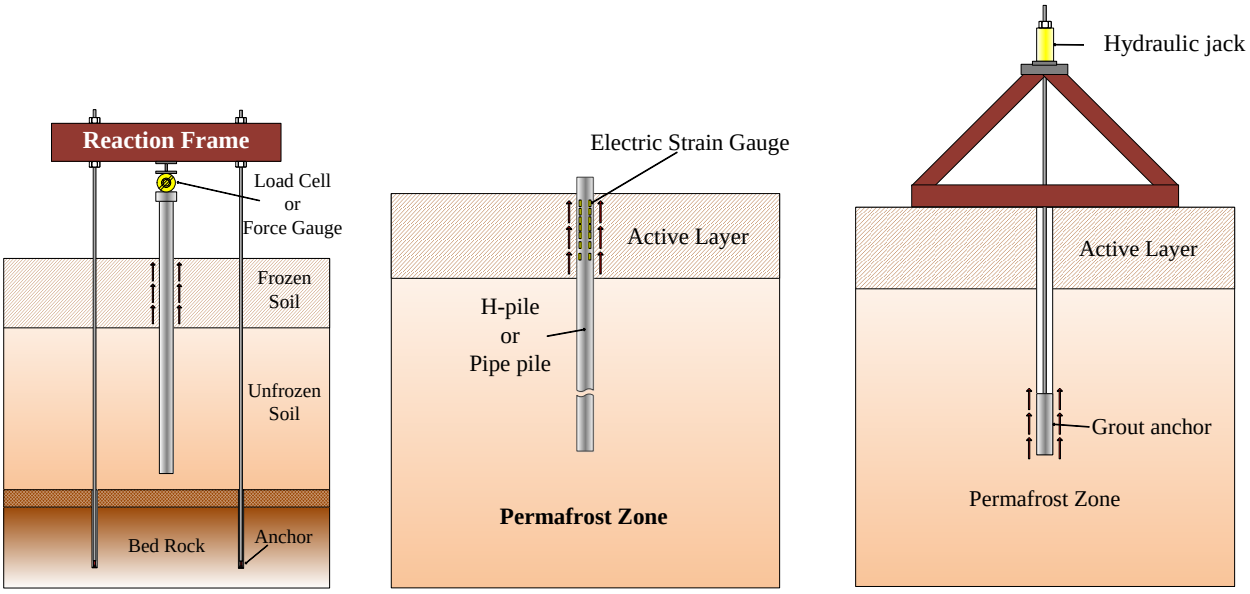

Figure 19. Various methods for measuring tangential heave forces: (a) reaction frame and load cell method (RFLCM), (b) strain gage method (SGM), and (c) pull-out or jack-in test method (POJIM) (after Kim et al. 2015)

3.2 TANGENTIAL HEAVE TEST SYSTEM

Tangential heave test system developed in this study mainly consisted of 1) environmental chamber, 2) 267-mm-wide box-type frost heave apparatus, 3) instrumented model pile, 4) data acquisition system, and 5) image acquisition system. To investigate developments of heave force along the pile, the research team used the strain gage method (SGM).

3.2.1 Instrumented model pile

The instrumented model pile was carefully designed to prevent any disturbance that may affect load transfer behavior of pile. Because the model pile is embedded in a fully saturated soil, a marine-grade stainless steel (Type 316) was selected as a pile material to minimize the corrosion during testing.

Two vertically cut circular piles with an identical diameter and a circular plate to cover the bottom of the pile were manufactured in a local machine shop (**Figure 20**(a)). On the inner surfaces of the piles, a total of 16 electrical resistance strain gages (Vishay Micro Measurement Model Name: CEA-06-250UN-350/P2), eight for each half pile, were installed (**Figure 20**(b)). Furthermore, a total of five thermocouples with hermetically sealed tip (Omega Engineering Model Name: HSTC-TT-T-20S-72-SMPW-CC) were installed on the inner surfaces of the piles. By installing these sensors on the inner surfaces of the pile, the entire outer surface of the pile is in direct contact with soil. This novel design minimizes the undesirable disturbance effect of the sensors on the pile-soil interactions that might have been present if they had been installed on outer surface of the pile.

After installing strain gages and thermocouples, inner joints of the two vertically cut piles were bonded using JB Water Weld Epoxy Putty (**Figure 20**(c)) and Loctite Marine Epoxy was applied onto the outer joints of the piles. All wires from the sensors were guided out through the top of the pile (**Figure 20**(d)). The bottom of the pile base was then covered with the circular base plate and bonded with the pile using Loctite Marine Epoxy to prevent water infiltration, forming a closed-ended pipe pile with an outer diameter of 48.3 mm with a wall thickness of 1.65 mm (**Figure 20**(e)). The Loctite Marine Epoxy was applied four more times on the joints to prevent any water from seeping into the pile (**Figure 20**(f)). After the epoxy had been cured, a waterproof test was conducted by submerging the pile into a water bucket for 12 hours and no water seepage into the pile was observed. To place the dial gage needle, a donut-shape alloy plate was attached to top of the pile. The inner space of the pile was sealed with a super absorbent polymer paper to protect the sensors inside the pile from moisture.

Figure 20. Photos showing instrumentations of model pile: (a) two vertically-cut piles and base cover plate, (b) installation of strain gages and thermocouple on the inner surfaces of the piles, (c) combination of the two piles, (d) guided wires through the pile top, (e) covering pile base with a circular plate, and (f) completed model pile

3.2.2 267-mm-wide box-type frost heave apparatus

The 267-mm-wide box-type frost heave apparatus was used for tangential heave testing. Due to its relatively large size, the soil box was able to accommodate the

instrumented model pile as well as other sensors. To measure the temperature variations across the soil depth, two thermocouples were installed in addition to the three Decagon 5TM moisture sensors. Instrumentation details of the soil box for tangential frost heave test including the model pile are presented in **Figure 21**.

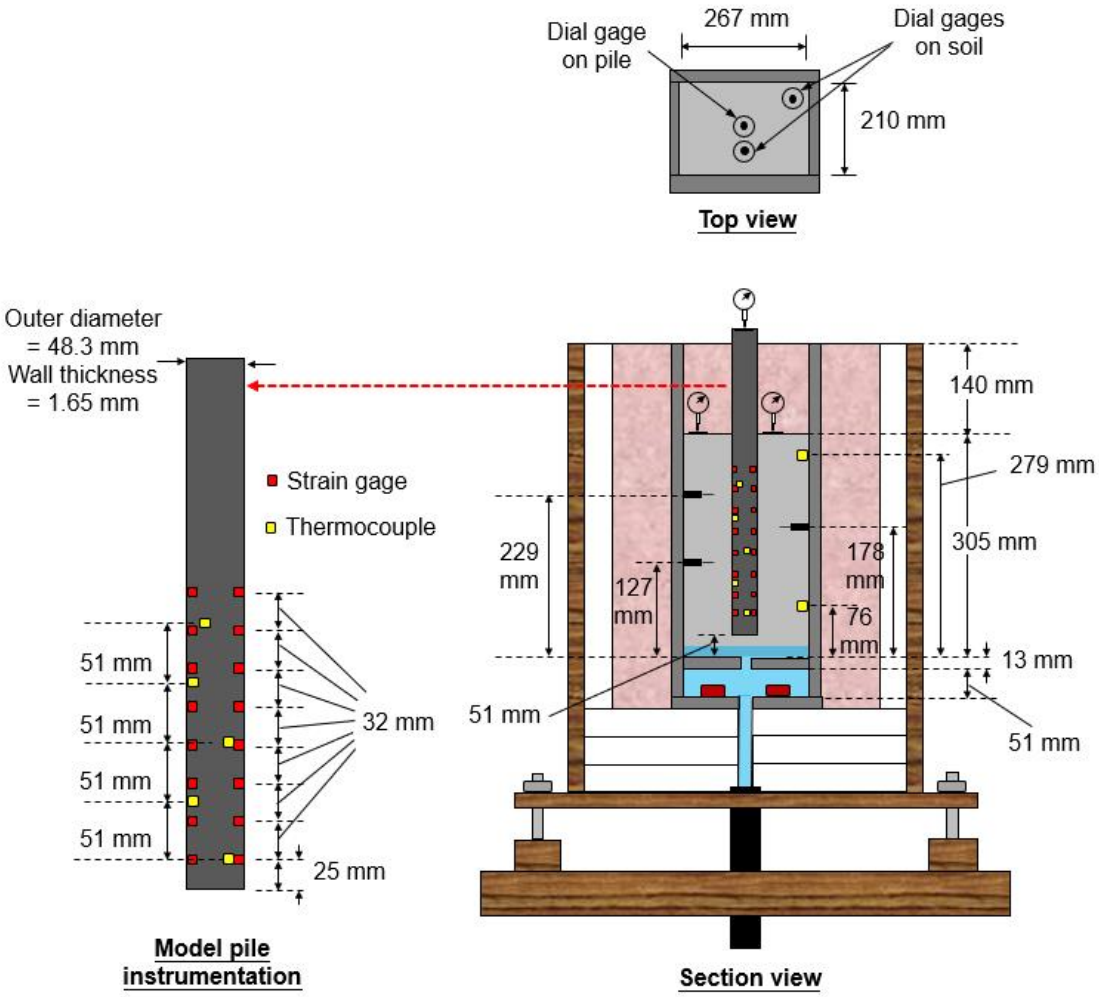

Figure 21. Instrumentation details of 267-mm-wide box-type apparatus with a model pile for tangential heave testing

3.2.3 Data acquisition system

All measurements from sensors were electronically taken using data acquisition system, except for dial gage readings. Strains and temperatures were collected using Vishay

Micro Measurement System 7000 data logger, and the water contents were collected using Decagon Device Em50 Data Logger. Strain, temperature, and moisture measurements were taken every 5 minutes. Dial gage readings were manually taken every hour until the first 12 hours and at least once per day thereafter.

3.2.4 Image acquisition system

As mentioned previously, the front panel of the soil box was made of Plexiglass to visually observe the soil sample. During the testing, the front panel was covered with an insulated wood door. When taking photos, the wood door was uncovered. A digital camera (Sony DSC-RX100) was placed about 400 mm in front of the front panel to record the images of soil sample during the testing. Three LED light sources with negligible heat generation were placed in front of the front panel for better lighting conditions (refer to **Figure 22**).

Figure 22. Photos of image acquisition system

3.3 TEST PROCEDURE

Experimental procedure for tangential heave test is very similar to that of frost heave test. The main difference is that, in tangential heave test, the instrumented model pile is embedded into the soil sample. Detailed test procedures for tangential heave test are as follows:

(1) Deposit test soil in the soil box until reaching 50 mm from the bottom of soil box (**Figure 23**(a)).

(2) Place the model pile and maintain its plumbness using a clamp and supports (**Figure 23**(b)).

(3) Add more soils until reaching the target elevation of the moisture sensor (or thermocouple) and place the moisture sensor (or thermocouple) (**Figure 23**(c)).

(4) Repeat Step (3) to install all three moisture sensors and two thermocouples.

(5) Add more soils until reaching a target height of soil sample (**Figure 23**(d)).

(6) Connect the water bath to constant-head water tank, remove the clamp and supports for the pile, and then saturate the soil sample.

(7) Connect the moisture sensors and strain gages with the data logger and place dial gages on the soil surface (**Figure 12**(e)) and pile top (**Figure 12**(f)).

(8) Set the target water temperature of the water bath using the temperature controller and heating device.

(9) Turn on the environmental chamber, set the target air temperature, and start running the test.

(10) Take dial gage readings and take photos of soil sample regularly.

(11) Run the test for target duration, then stop the test.

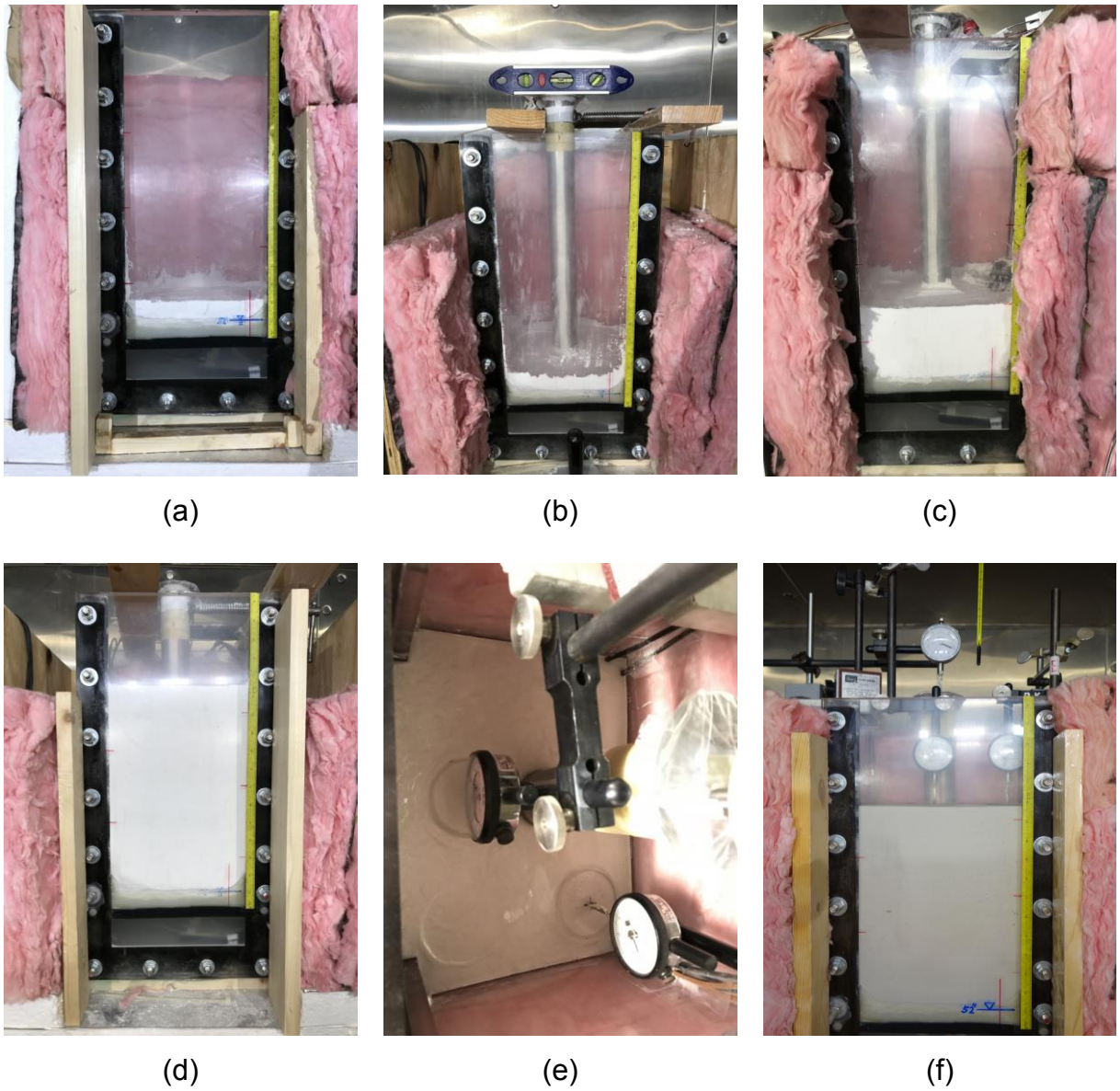

Figure 23. Photos showing tangential heave test procedures: (a) deposition of test soil in a soil box, (b) placement of a model pile, (c) installation of moisture sensors (or thermocouples), (d) completion of soil deposition, (e) installation of dial gages on soil, and (f) installation of a dial gage on pile top

After completion of the saturation process, the height of soil sample at the start of frost heave testing was 295 mm. Also, when the clamp and supports were removed from the pile and the saturation process began, pile head settlement was observed due to self weight of the pile, achieving a total settlement of 28.3 mm by the end of the saturation process. Therefore, at the start of frost heave testing, the distance between the pile base and bottom of soil sample was 22.5 m. Air temperature of the environmental

chamber was set to –10 °C and the water temperatures in the bath set to be 15 °C, corresponding to a temperature gradient of 0.082°C/mm between the top and bottom of the soil sample.

3.4 TEST RESULTS

3.4.1 Heave amounts

Amounts of frost heave measured at the center of the soil surface, at the corner of the soil surface, and at the pile top are presented in **Figure 24**. Initially, slightly greater heave was observed at the corner than at the center of the soil surface, but after about 28 hours the center of the soil surface heaved more than the corner. At around 250 hours after the test began, the heave amounts at the center and corner of the soil surface were stabilized at 18 mm and 14 mm, respectively.

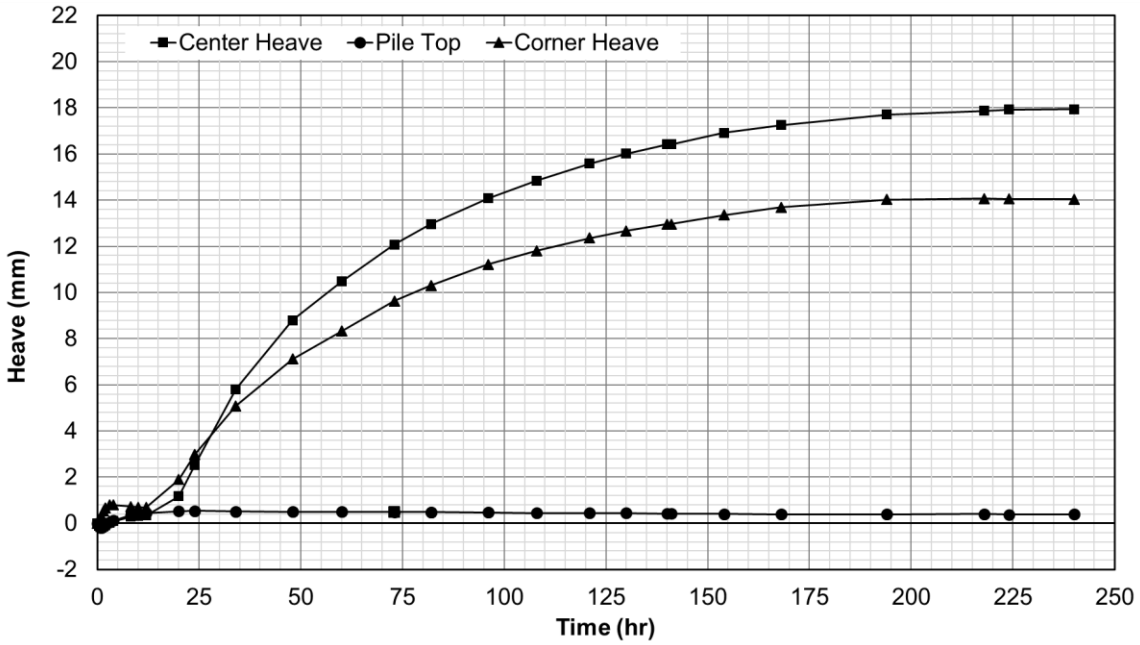

(a)

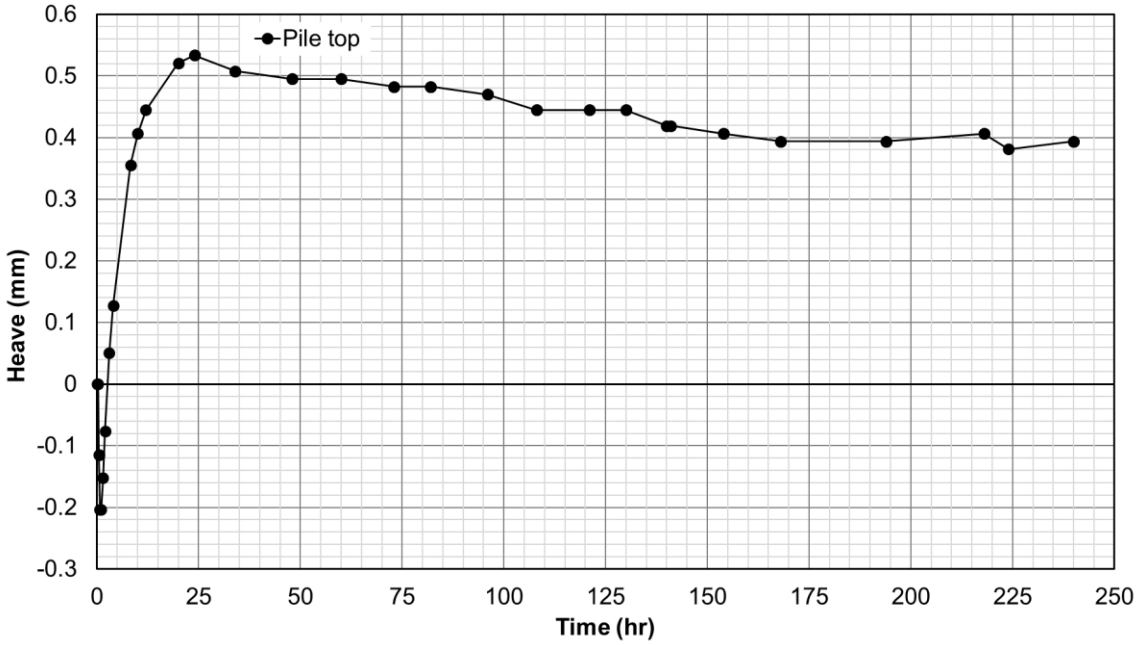

(b)

Figure 24. (a) Amounts of soil heave measured at the center and corner of the soil surface and pile movement versus time and (b) pile top movement only (testing conditions: air temperature of environmental chamber = –10 °C; water temperature in water bath = 15 °C; temperature gradient = 0.085°C/mm; test soil = SIL-CO-SIL-250)

The pile top initially settled until reaching 1 hour after the test began, but then it started moving upward and reached a peak upward movement of 0.533 mm at 24 hours. After 24 hours, no significant pile top movement was observed. The frost heave rates at the center of the soil surface about every 24 hours until reaching until 312 hours are presented in **Table 5**.

Table 5. Frost heave rates at the center of soil surface about every 24 hours until reaching 312 hours from tangential heave test

Time (hour)	Pile top movement (mm)	Soil heave at center (mm)	Soil heave rate (mm/day)	Soil heave rate (mm/hr)
0	0	0	-	-
24	0.533	2.527	2.527	0.1053
48	0.495	8.801	6.274	0.2614
73	0.483	12.078	3.277	0.1311
96	0.470	14.084	2.006	0.0872
121	0.445	15.583	1.499	0.0600
141	0.419	16.421	0.838	0.0419
168	0.406	16.916	0.495	0.0183
194	0.394	17.704	0.788	0.0303
218	0.406	17.869	0.165	0.0069
248	0.381	17.971	0.102	0.0034
266	0.419	17.920	-0.051	-0.0028
288	0.445	17.869	-0.051	-0.0023
312	0.432	17.793	-0.076	-0.0032

3.4.2 Observations of sample images during test

Figure 25 shows images of soil sample taken during the tangential heave test. A center of the soil surface heaved by about 8.8 mm at 48 hours, but no ice lens was observed until then. The first ice lens appeared 60 hours after the test begun, and afterward new ice lenses was observed about every 12 hours until 96 hours. Furthermore, newer ice lenses were formed below the old ice lenses. At 192 hours, a total of six ice lenses were observed and no additional new ice lenses were formed thereafter.

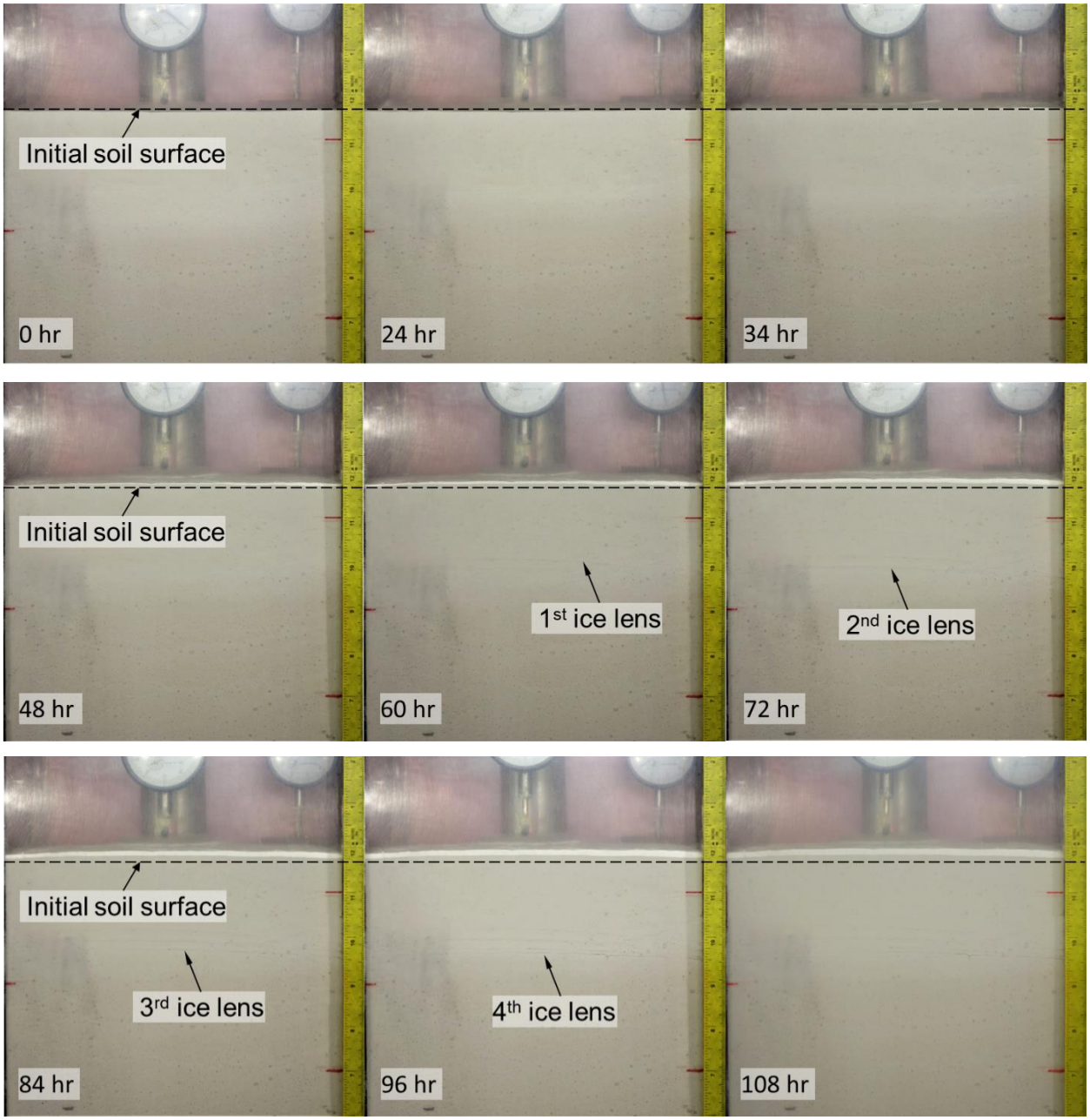
Initial soil surface
0 hr
24 hr
34 hr
Initial soil surface
1st ice lens
2nd ice lens
48 hr
60 hr
72 hr
Initial soil surface
3rd ice lens
4th ice lens
84 hr
96 hr
108 hr

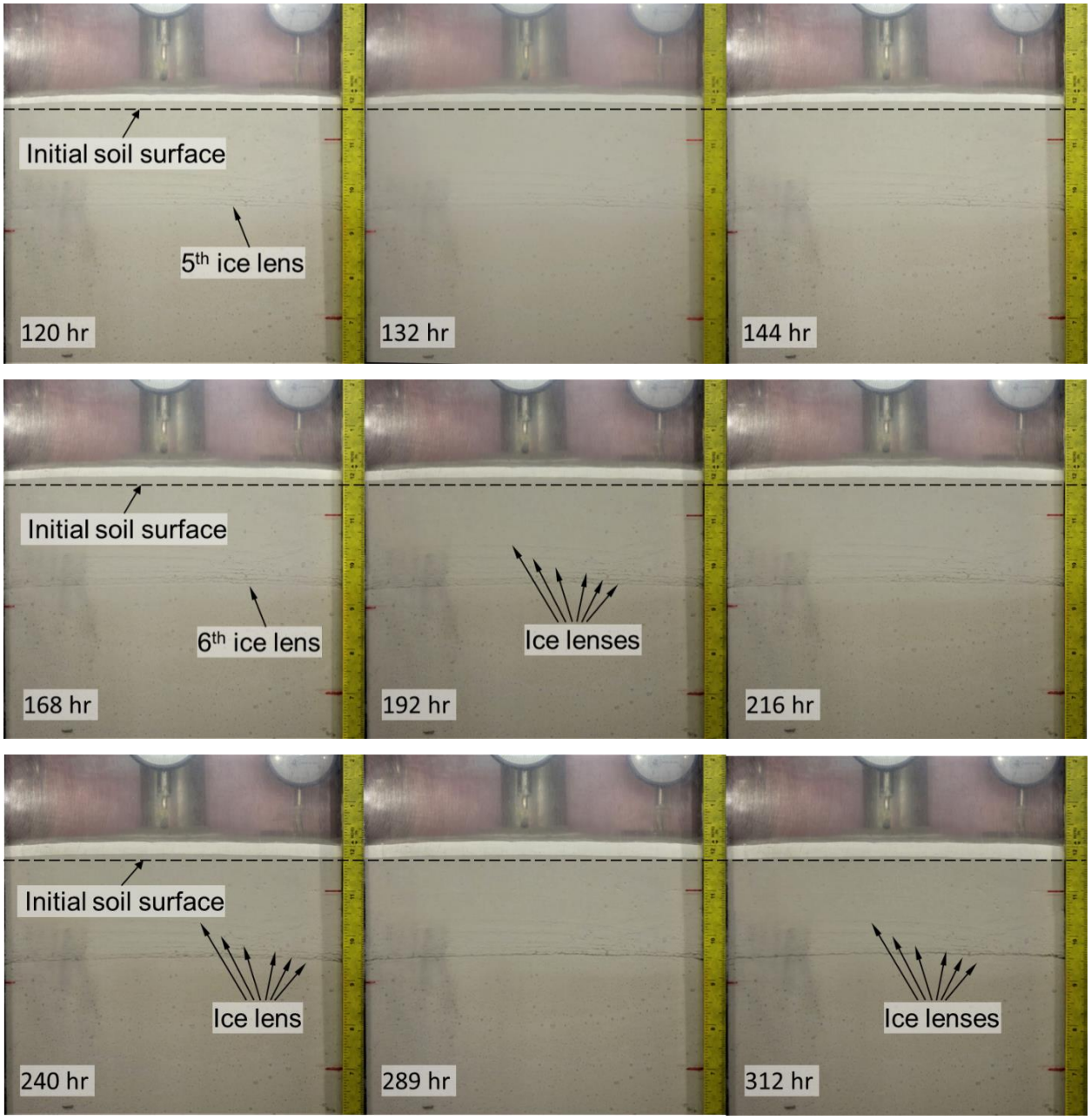

Figure 25. Images of soil sample during tangential heave test taken at various elapsed times (testing conditions: air temperature of environmental chamber = –10 °C; water temperature in water bath = 15 °C; temperature gradient = 0.085°C/mm; test soil = SIL-CO-SIL-250)

3.4.3 Temperature variations

Figure 26(a) shows variations of soil temperature, measured from the built-in thermistor of the three moisture sensors and two thermocouples, versus elapsed time.

Temperature measurements were taken at locations of 76, 127, 178, 229, and 279 mm above the bottom of soil sample. Similarly, **Figure 26**(b) shows variations of pile temperature, measured from the thermocouples installed on the inner surface of the pile, versus elapsed time. Both plots suggest that the thermal equilibrium condition was achieved at about 70 hours after the test began.

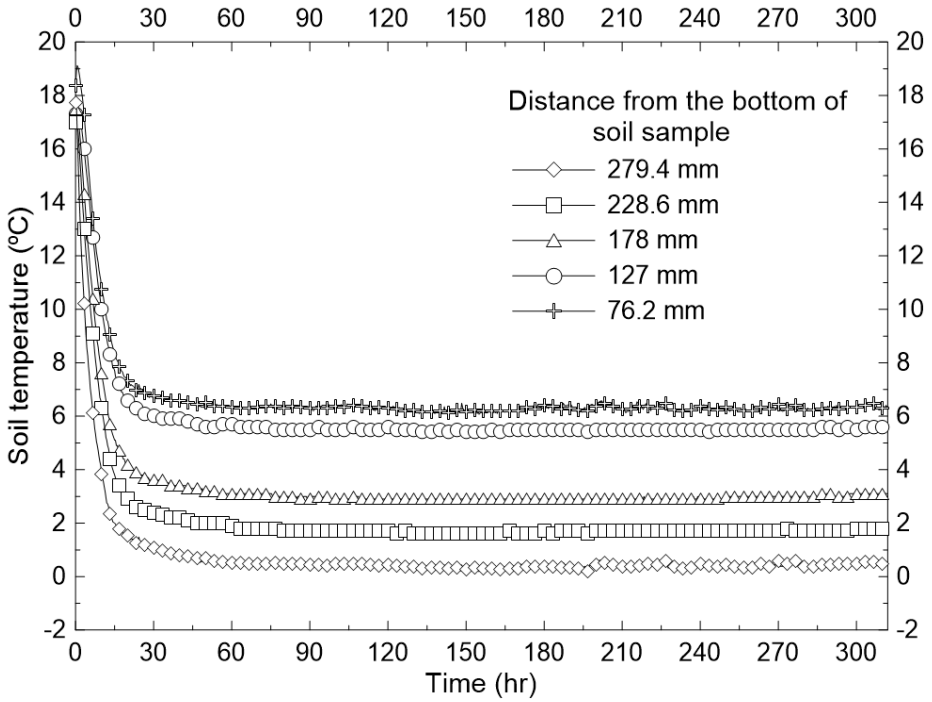

(a)

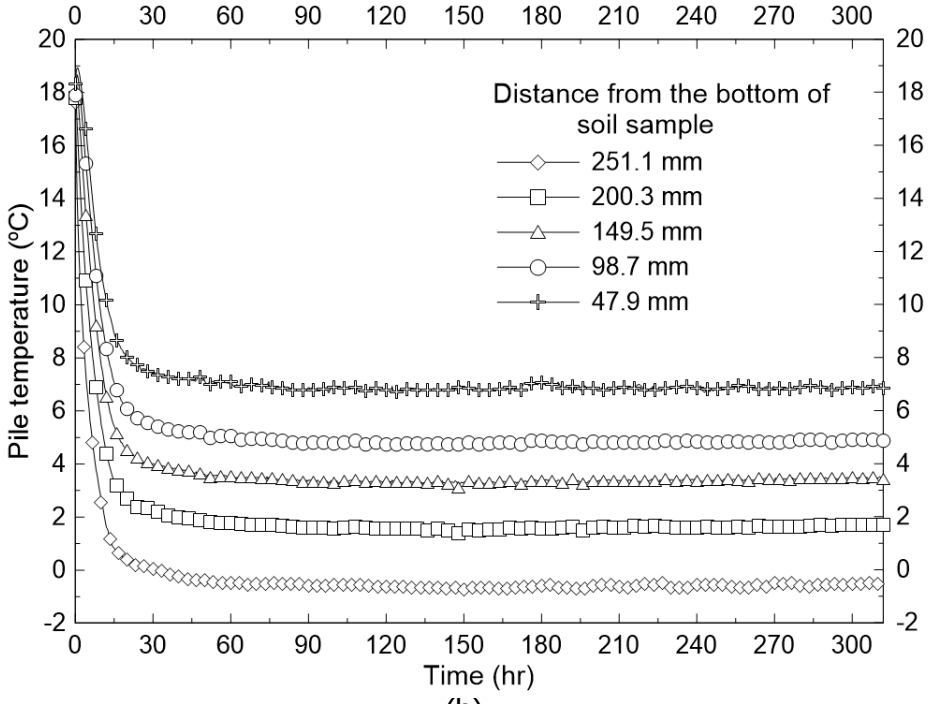

(b)

Figure 26. (a) Soil temperature versus time and (b) pile temperature versus time (testing conditions: air temperature of environmental chamber = –10 °C; water temperature in water bath = 15 °C; temperature gradient = 0.085°C/mm; test soil = SIL-CO-SIL-250)

Figure 27 shows the temperature versus distance from the bottom of soil sample at various elapsed times measured from moisture sensors and thermocouples embedded in soil (**Figure 27**(a)) and measured from thermocouples installed on inner surface of the pile (**Figure 27**(b)). As seen previously, soil temperatures decreased with increasing time until reaching 72 hours but no changes were observed thereafter (refer to **Figure 27**(a)). The temperature profile measured from thermocouples inside the pile showed similar trend (refer to **Figure 27**(b)). It should be noted that the locations of the actual moisture sensors and thermocouples embedded in the soil may be a bit lower than the depths shown in **Figure 27**(a) because the soil sample underwent settlement during saturation process. Furthermore, the sensors embedded in the soil were located near the wall of the soil box, not at the center of the tank where the pile is located. Therefore, the research team believes that the pile temperature profiles shown in **Figure 27**(b) better represent the actual soil temperature in the vicinity of the pile. **Figure 27**(b) suggest that the frost depth was located at about 235 mm above the bottom of the soil sample.

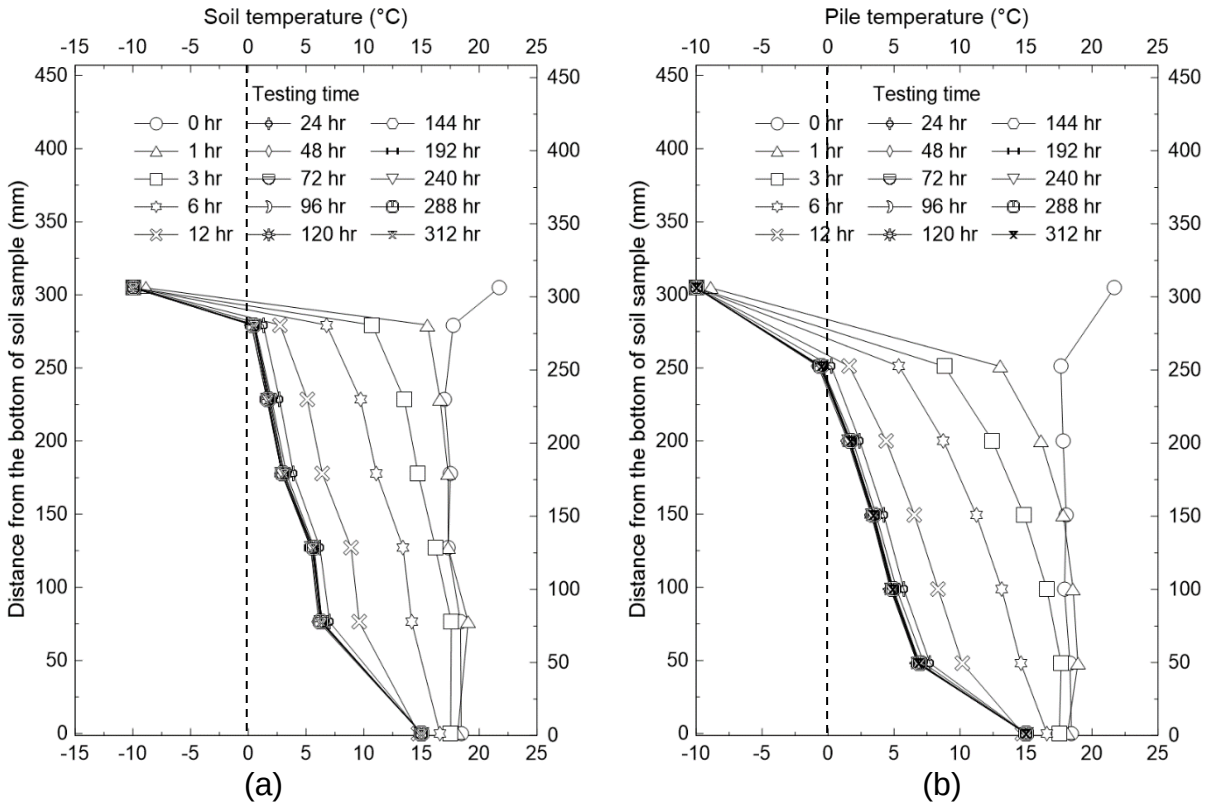

Figure 27. (a) Soil temperature and (b) pile temperature versus distance from the bottom of the soil sample at various elapsed times (testing conditions: air temperature of environmental chamber = –10 °C; water temperature in water bath = 15 °C; temperature gradient = 0.085°C/mm; test soil = SIL-CO-SIL-250)

3.4.4 Moisture content variations

Figure 28 shows variations of volumetric water content measured from the three moisture sensors versus elapsed time, and **Figure 29** shows volumetric water contents versus depth at various elapsed times. In the beginning of the test, the volumetric water contents from all sensors showed slight increase up to about 20 hours, but after that no significant change was observed.

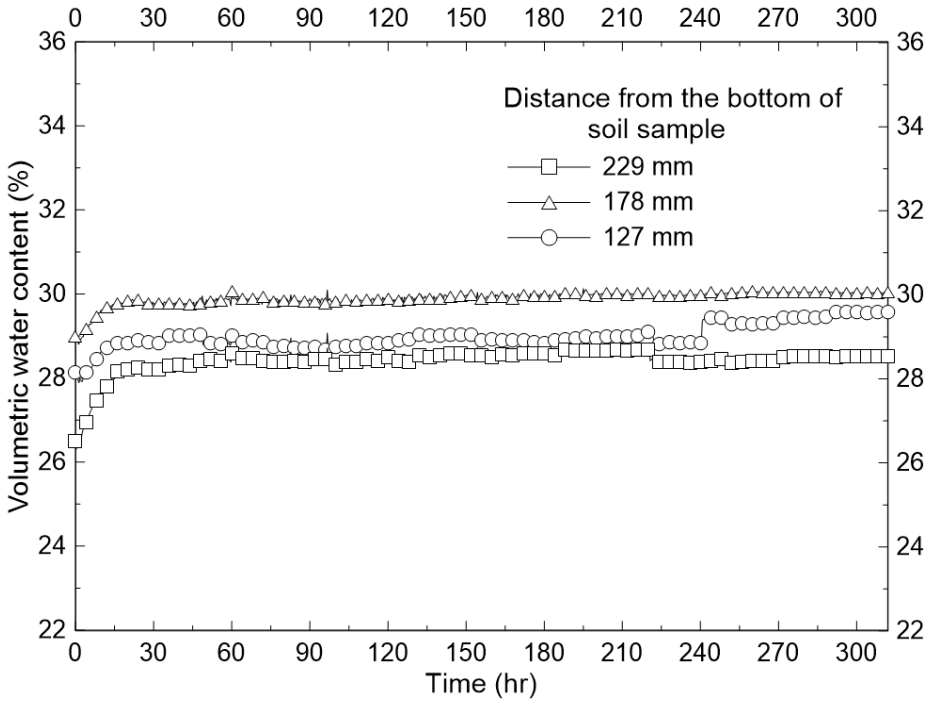

Figure 28. Volumetric water content at various depths of soil sample versus time (testing conditions: air temperature of environmental chamber = –10 °C; water temperature in water bath = 15 °C; temperature gradient = 0.085°C/mm; test soil = SIL-CO-SIL-250)

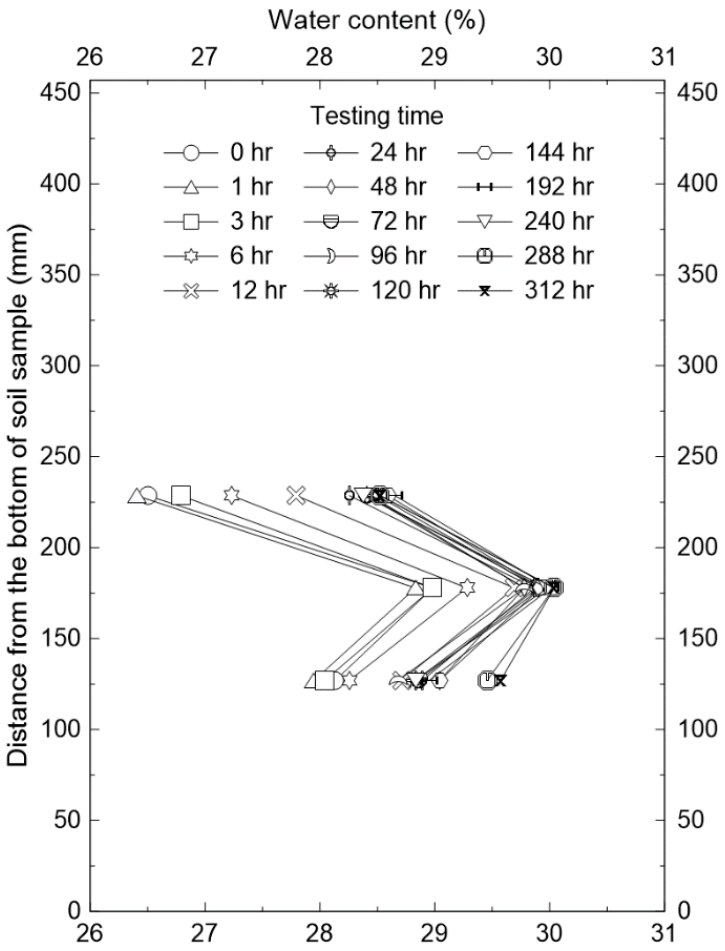

Figure 29. Volumetric water content versus distance from the bottom of the soil sample at various elapsed times (testing conditions: air temperature of environmental chamber = –10 °C; water temperature in water bath = 15 °C; temperature gradient = 0.082°C/mm; test soil = SIL-CO-SIL-250)

3.4.5 Strains in pile

Measured strains

As mentioned previously, a total of 16 strain gages, eight on each half pile, were instrumented on the test pile. However, all eight strain gages on one side of the pile showed erratic and unreliable data and, therefore, were not used in data interpretation. Furthermore, two additional strain gages on the other side of the pile showed erroneous readings and were deemed unusable. Accordingly, the remaining six strain gages that showed stable readings throughout the testing duration were used in interpretations of the test results. **Figure 30** shows distribution of axial strains measured from the six

strain gages versus elapsed time. **Figure 31** shows the axial strain versus depth at various elapsed times as well as the elevations of the initial and final surfaces of the soil sample. The location of the deepest ice lens visually observed in the soil sample is also shown in the figure.

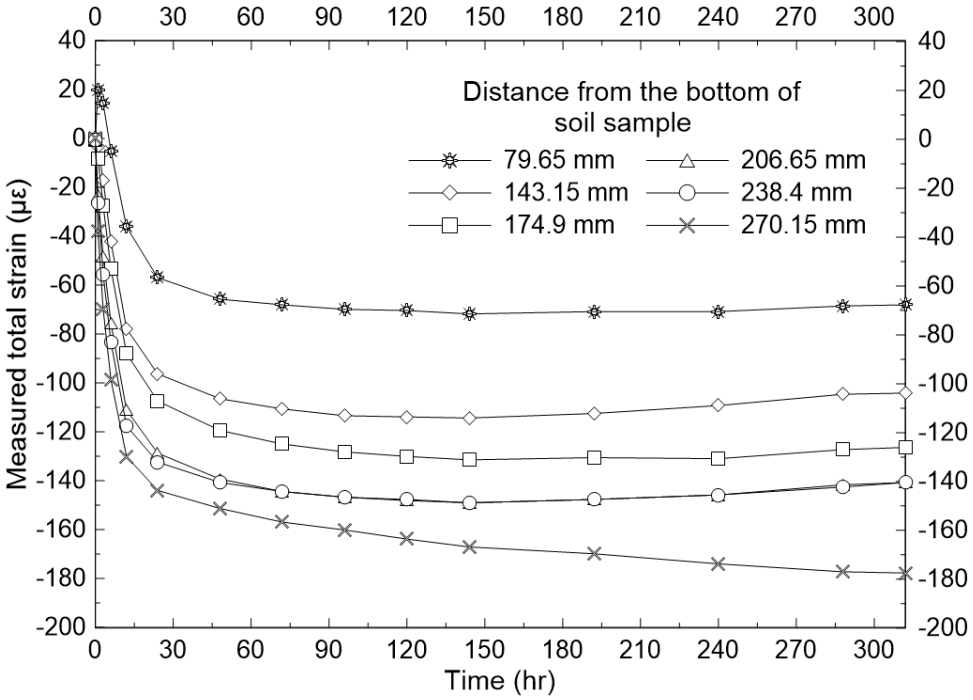

Figure 30. Axial strains in pile at various depths versus time (testing conditions: air temperature of environmental chamber = –10 °C; water temperature in water bath = 15 °C; temperature gradient = 0.085°C/mm; test soil = SIL-CO-SIL-250)

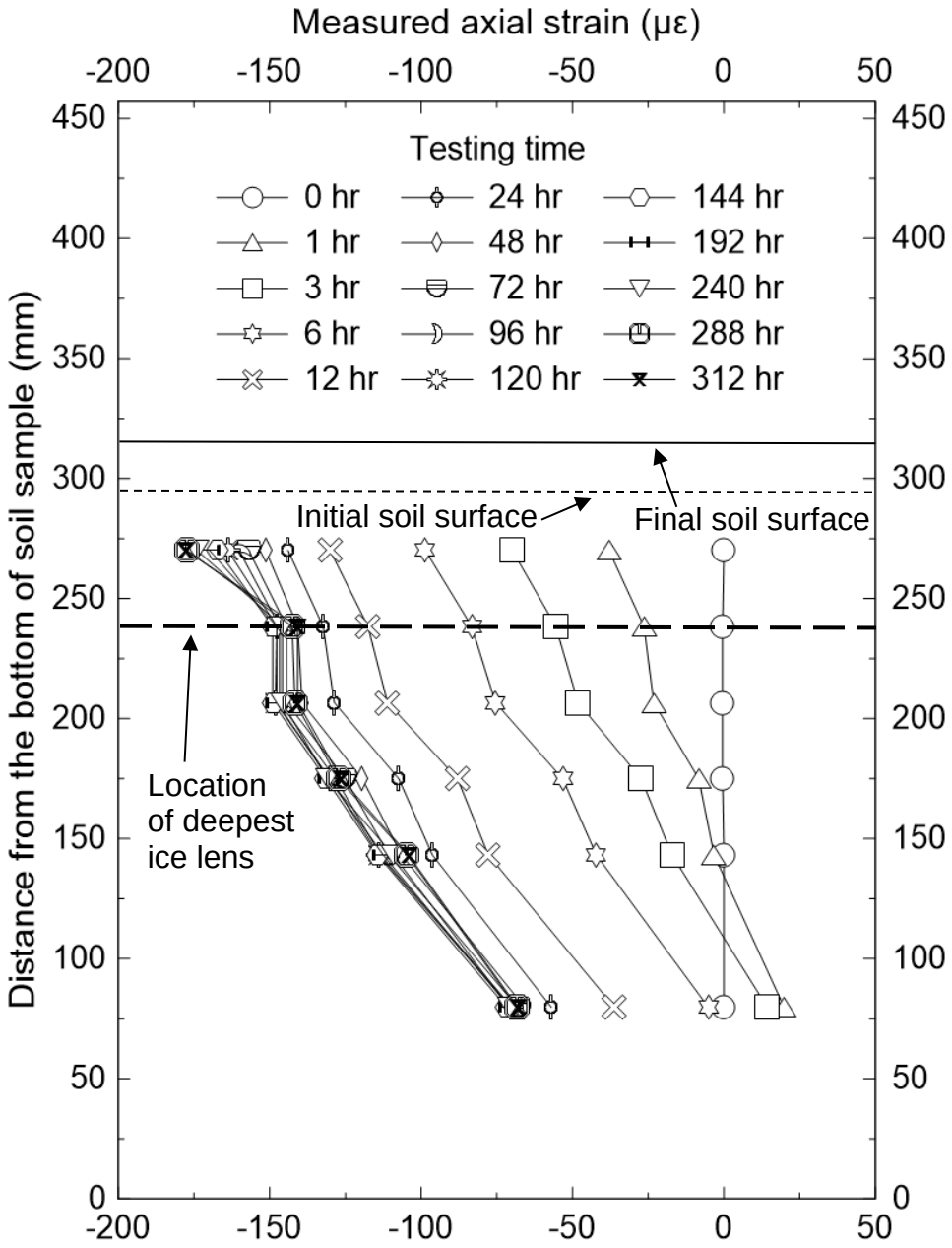

Figure 31. Axial strains in pile versus distance from the bottom of the soil sample at various elapsed times (testing conditions: air temperature of environmental chamber = –10 °C; water temperature in water bath = 15 °C; temperature gradient = 0.085°C/mm; test soil = SIL-CO-SIL-250)

Thermally induced strains

During the tangential heave test, two types of strain develop in pile: (a) thermally induced strain by the temperature change of the pile and (b) mechanically induced strain due to heaving soil. In order to determine the mechanically induced strains by the

heaving soil, the thermally induced strains need to been eliminated from the measured axial strains.

To calculate thermally induced strain, the research team determined the coefficient of thermal expansion α of the test pile from a separate test. After the tangential heave test was completed, the soil box was emptied and the test pile was vertically placed inside the box without any soil. Strain values were zeroed at the initial room temperature of 20 °C, and then the air temperature of the environmental chamber was set to -12 °C. The test for measurement of thermal expansion coefficient was run for about 320 hours and changes in strains and pile temperatures were electronically recorded during the testing period.

The thermal expansion coefficient α was determined by first plotting change in temperature (ΔT) versus change in strain ($\Delta\varepsilon$) obtained from the separate test and then determining the slope of the best fitted line going through the origin. **Figure 32** shows an example of such process using the strain gage located about 80 mm above from the bottom of the soil sample. Ideally, the thermal expansion coefficient of the test pile material should be represented by a single value of α. However, strain gages may not have been perfectly aligned and each strain gage may have a different amount of offset from the vertical alignment. Furthermore, the use of epoxy bond to combine the two vertical pipes may have locally altered the material property of the test pile as a composite. Therefore, in this project, the value of α was determined for each strain gage location. **Table 6** shows the coefficients of thermal expansion of the test pile at each strain gages locations, and the values of α vary from 8.2 to 9.5 micro-strain/°C.

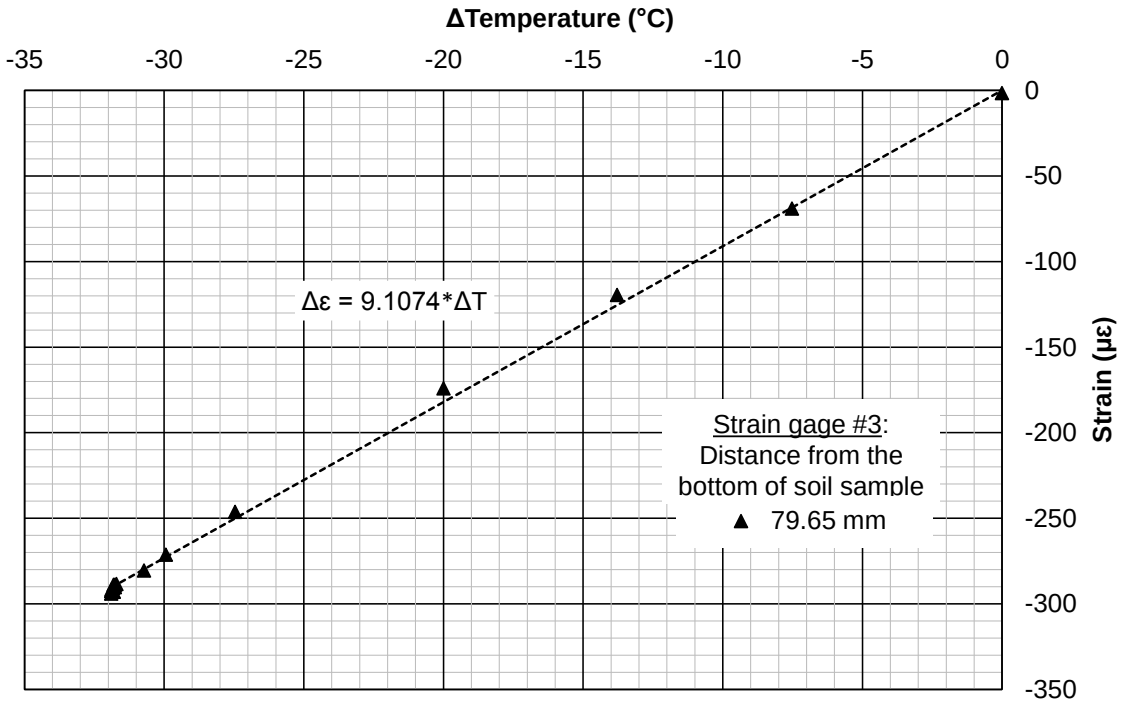

Figure 32. Determination of coefficient of thermal expansion of the test pile at the strain gage location (Strain Gage #3 located at 79.65 mm above from the bottom of soil as an example)

Table 6. Coefficients of thermal expansion at each strain gages locations

Strain gage number	Distance from the bottom of soil sample (mm)	Coefficient of thermal expansion (με/°C)
3	79.65	9.1
7	143.15	8.8
9	174.9	8.2
11	206.65	9.5
13	238.4	9.3
15	270.15	9.0

Since the values of thermal expansion coefficient α at each strain gage locations were determined from a separate test, thermally induced strains at any given temperature can be easily computed from the relationship of $\Delta\varepsilon = \alpha(\Delta T)$. **Figure 33** shows thermally induced strains versus elapsed time obtained from the tangential heave test using the

thermal expansion coefficient α and temperature of the pile at each strain gage locations. **Figure 34** shows thermally induced strain in pile versus distance from the bottom of the soil sample at various elapsed times.

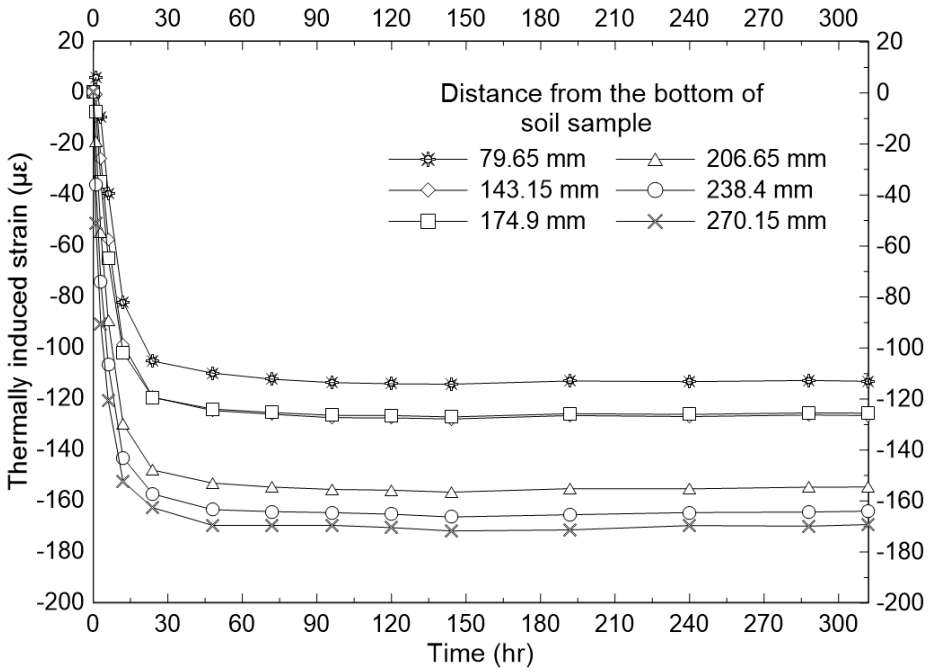

Figure 33. Thermally induced strains in pile at various depths versus time (testing conditions: air temperature of environmental chamber = –10 °C; water temperature in water bath = 15 °C; temperature gradient = 0.085°C/mm; test soil = SIL-CO-SIL-250)

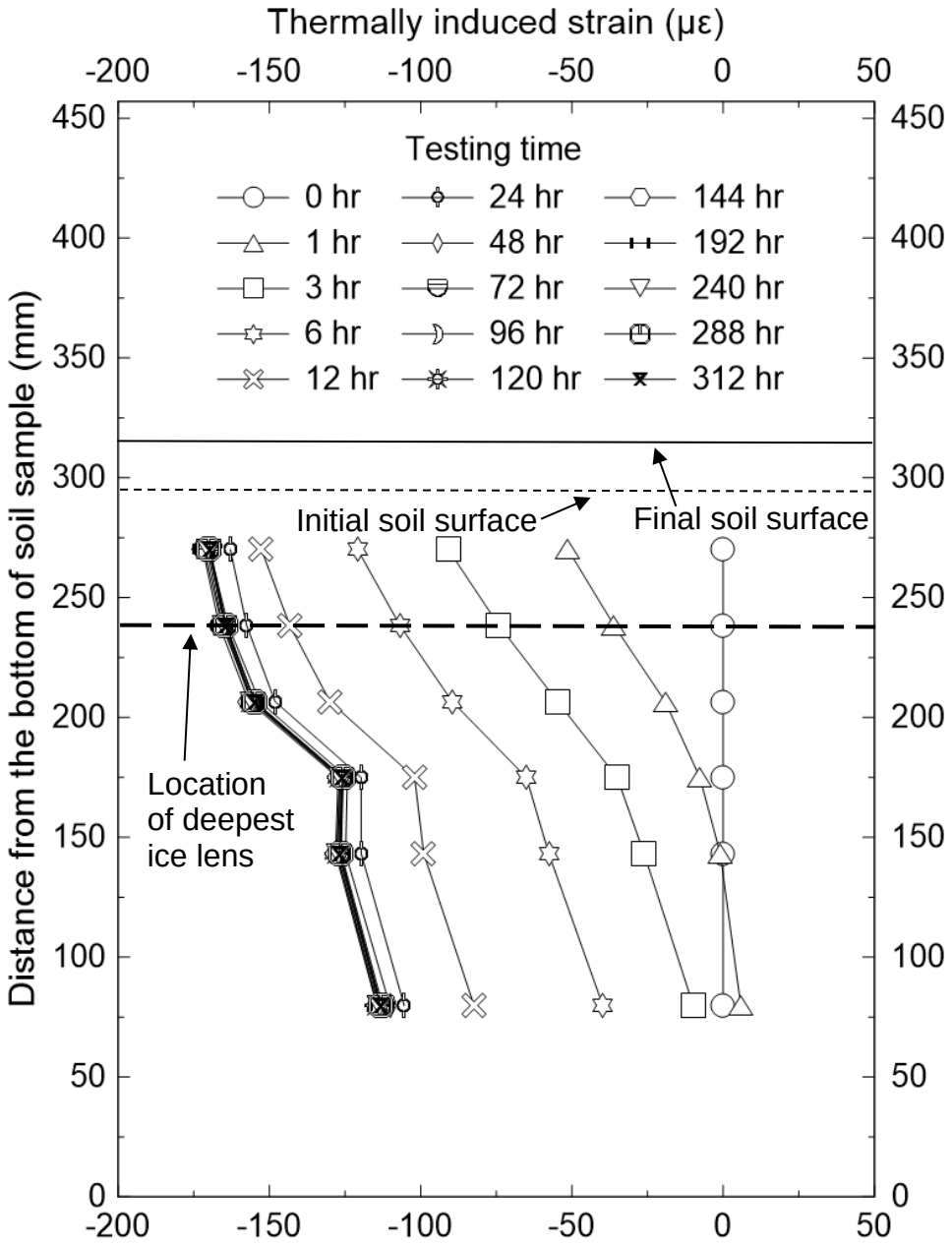

Figure 34. Thermally induced strain in pile versus distance from the bottom of the soil sample at various elapsed times (testing conditions: air temperature of environmental chamber = –10 °C; water temperature in water bath = 15 °C; temperature gradient = 0.085°C/mm; test soil = SIL-CO-SIL-250)

Mechanically induced strains

Mechanically induced strains were obtained by subtracting the thermally induced strains from the measured strains for each strain gage. Then, the axial forces acting on the pile

resulted from the frost heave during soil freezing was determined by multiplying the mechanical strains by the pile stiffness E_pA_p (Young's modulus E_p of the test pile was assumed to be 200 GPa). **Figure 35** shows mechanically induced strain on the right vertical axis and axial force on the left vertical axis versus time. Similarly, **Figure 36** shows mechanical strains on the bottom horizontal axis and axial forces on the top horizontal axis versus distance from the bottom of the soil sample at various elapsed times.

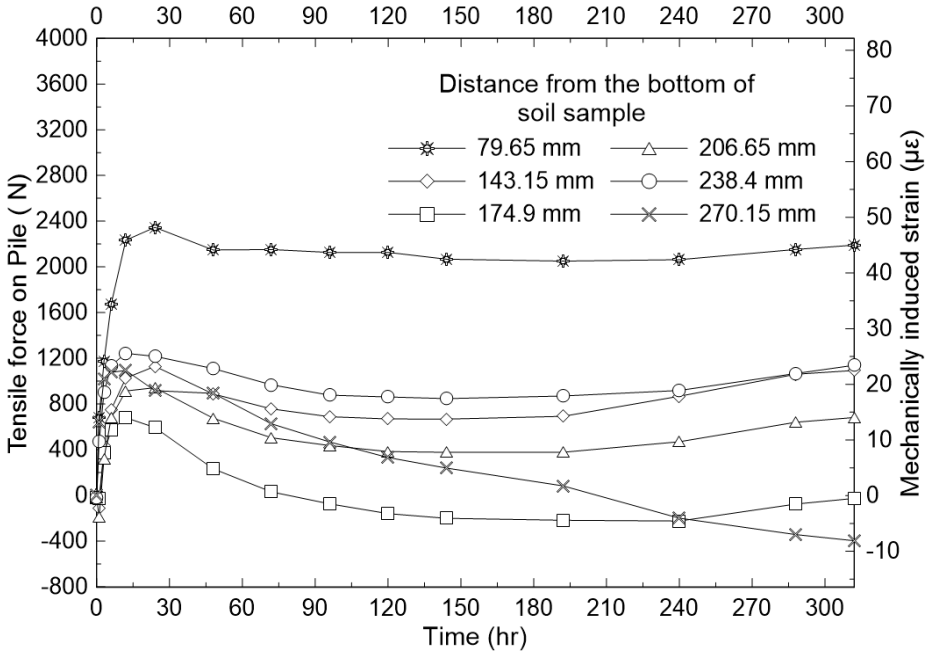

Figure 35. Mechanically induced strains and axial forces on pile at various depths versus time (testing conditions: air temperature of environmental chamber = –10 °C; water temperature in water bath = 15 °C; temperature gradient = 0.085°C/mm; test soil = SIL-CO-SIL-250)

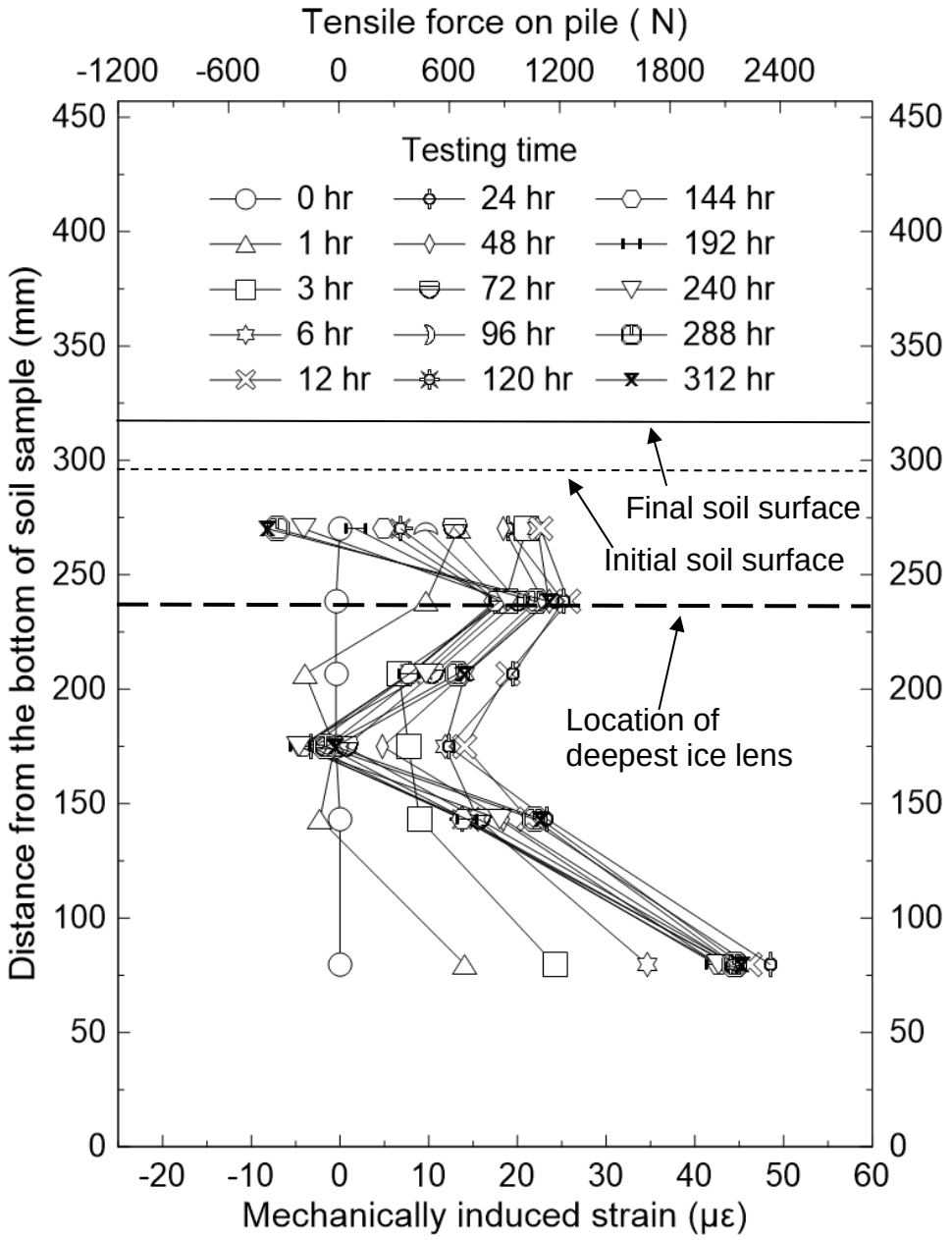

Figure 36. Mechanically induced strains and axial forces on pile versus distance from the bottom of the soil sample at various elapsed times (testing conditions: air temperature of environmental chamber = –10 °C; water temperature in water bath = 15 °C; temperature gradient = 0.085°C/mm; test soil = SIL-CO-SIL-250)

3.4.6 Tangential heave stress

This section presents the development of tangential heave stress versus time. The tangential heave stress (or uplift shear stress) was computed by dividing the axial force Q_f at the frost depth d_f by the outer surface area of the pile from the ground surface to the frost depth (refer to **Figure 37**). The axial force on pile at the ground surface was assumed to be zero because there is no confining sress there.

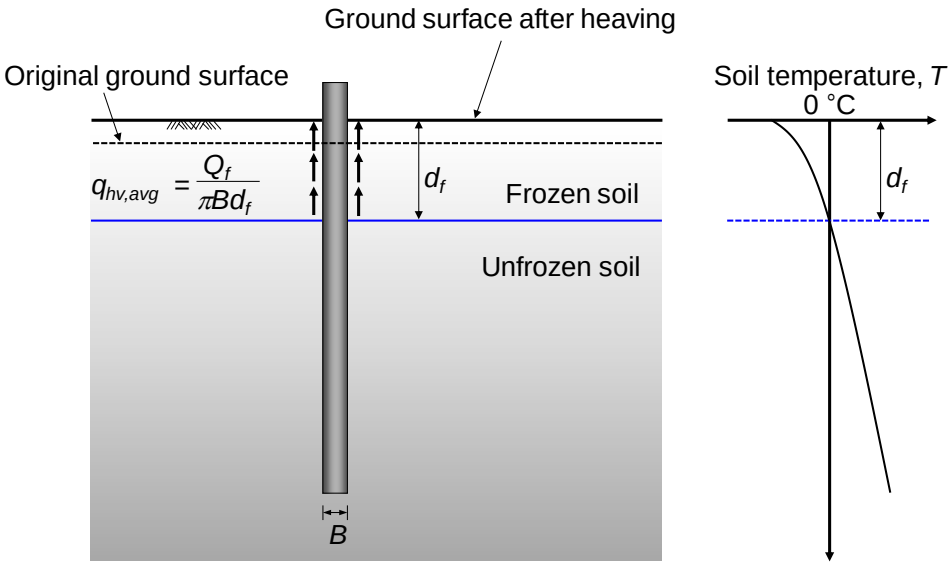

Figure 37. Conceptual sketch illustrating the behavior of deep foundation during frost heave

The frost depth d_f versus time was determined by first identifying the depth of the 0 °C isotherm using the pile temperature profiles shown in **Figure 27**(b) and then adding the amount of soil heave at the center of the soil surface shown in **Figure 24**(a). On the other hand, the axial force Q_f at the frost depth was interpolated using the axial force profile data shown in **Figure 36**. Then, the average tangential heave stress $q_{hv,avg}$ an any given time was computed as follows:

$$q_{hv,avg} = \frac{Q_f}{\pi B d_f} \quad (1)$$

Figure 38 shows the $q_{hv,avg}$ and d_f versus time obtained from this study. The frost depth d_f gradually increased with time and eventually converged to a depth of about 75 mm below the ground surface (corresponding to the distance of 236 mm from the bottom of the soil sample). On the other hand, the tangential heave stress sharply increased at the very early stages of the test and showed a peak value of about 280 kPa at elapsed time of 6 hr. After that, the $q_{hv,avg}$ drastically decreased and achieved a minimum value of about 66 kPa at 144 hr. At the end of the testing at 312 hr, the value of $q_{hv,avg}$ was about 100 kPa. As seen previously in **Figure 24**, the soil continuously heaved until reaching about 250 hours, whereas the pile stopped heaving at 24 hr. This indicates that the slippage between the pile and soil happened due to the breakage of the adfreeze bond between the pile and soil and is attributed to the drastic decrease of $q_{hv,avg}$ after initial sharp increase.

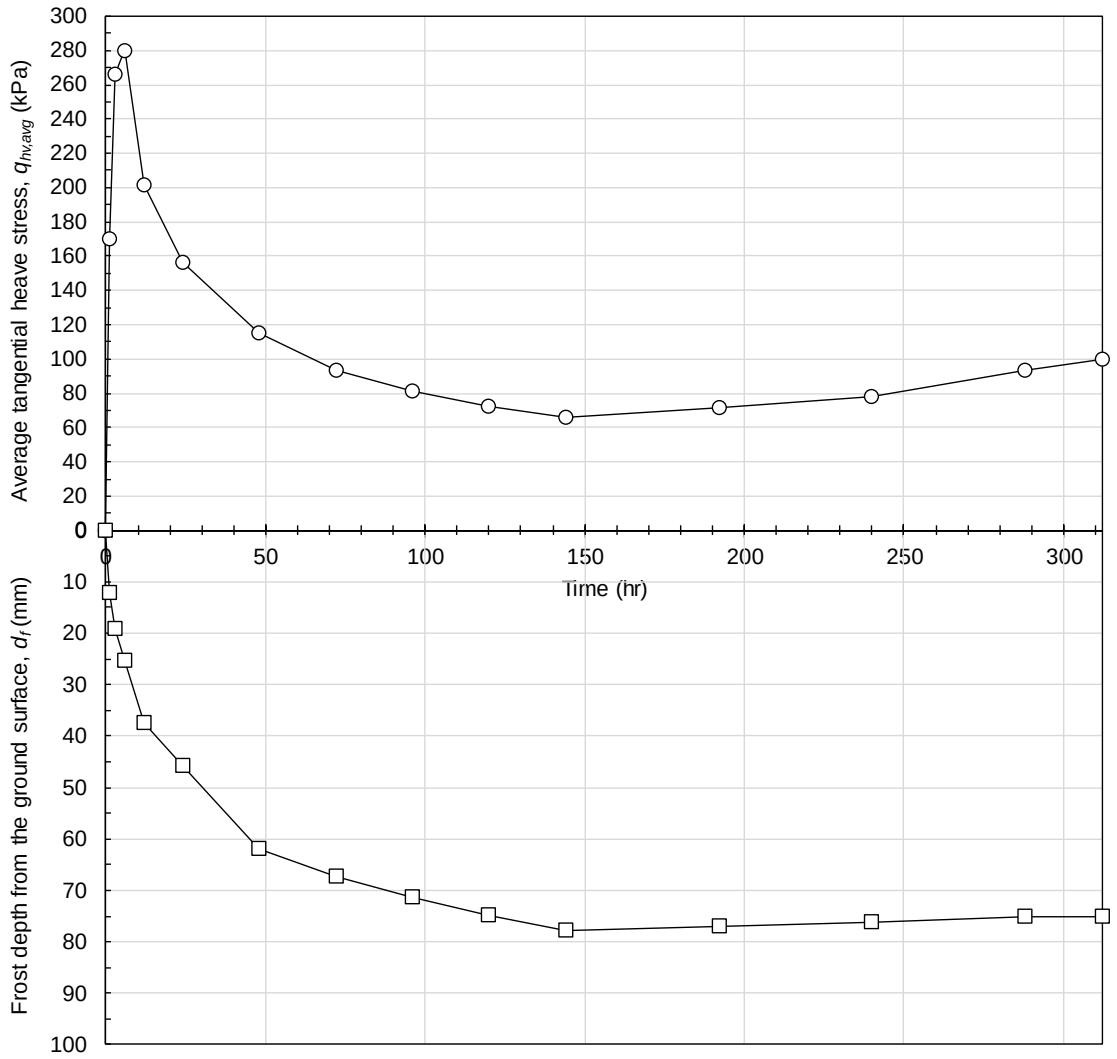

Figure 38. Average tangential heave stress acting on the pile (testing conditions: air temperature of environmental chamber = –10 °C; water temperature in water bath = 15 °C; temperature gradient = 0.085°C/mm; test soil = SIL-CO-SIL-250)

4. SUMMARY AND CONCLUSION

This study investigated the effect of frost heave during soil freezing on the development of tangential heave force on deep foundations. To achieve the research objectives, two different frost heave test apparatuses were developed: (1) a 76-mm-diameter cylinder-type apparatus and (2) a 267-mm-wide box-type apparatus. The 76-mm-diameter cylindrical apparatus was easy to build and enabled the research team to assess frost-susceptibility of various soil types simultaneously. The 267-mm-wide box apparatus not only successfully simulated frost heave process in a larger scale but also provided various experimental data such as soil temperature, soil moisture, heave amount, and images of ice lens formation process during frost heave testing.

The 267-mm-wide box-type frost heave apparatus was further used for tangential heave testing. Due to its relatively large size, the soil box was able to accommodate a model pile as well as moisture sensors and thermocouples. The model pile was customarily manufactured by bonding two vertically-cut half piles into a single, closed ended pipe pile. Strain gages and thermocouples were installed on inner surfaces of the pile before bonding to minimize disturbances on pile-soil interactions.

The instrumented model pile was embedded in the testing soil, and a total height of 295 mm of soil sample, after saturation, was deposited for tangential heave testing. Air temperature of the environmental chamber was set to –10 °C and the water temperatures in the bath set to be 15 °C, corresponding to a temperature gradient of 0.082°C/mm between the top and bottom of the soil sample. At 194 hours after the test began, a total of six ice lenses were observed and no additional new ice lenses were formed thereafter. The maximum the heave amounts at the center and corner of the soil surface were 18 mm and 14 mm, respectively, at about 250 hours. The pile top reached a peak upward movement of 0.533 mm at 24 hours, and no significant change was observed thereafter.

Axial strains developed in the pile during the tangential heave testing were successfully measured. Thermal expansion coefficients of the pile at each location of the strain gage were determined from a separate test, and the thermally induced strains were then computed using the measured thermal expansion coefficients. Mechanical strains induced by the heaving soil were obtained by subtracting the thermally induced strains from the measured strains. The mechanically induced strains were then converted into axial forces using the pile stiffness. From the axial force distribution above the frost depth, an average tangential heave stress was computed. The average tangential heave stress sharply increased at the very early stages of the test and showed a peak value of about 280 kPa at an elapsed time of 6 hr. After that, the $q_{hv,avg}$ drastically decreased and achieved a minimum value of about 66 kPa at 144 hr. At the end of the testing at 312 hr, the value of $q_{hv,avg}$ was about 100 kPa.

The tangential heave tests using an instrumented model pile and image acquisition system produced a wealth of information that can improve fundamental understanding of ice-soil-pile interaction. In particular, given the absence of standard test methods to assess tangential heave stress during soil freezing, the testing system and procedure developed in this study may contribute to establish a standard test method to evaluate tangential heave stress acting on deep foundations during frost heave. Furthermore, experimental study for various temperature gradients and structural loads on the pile, that can be done as a future study using the developed testing system, can make a significant contribution to the body of knowledge for foundation design in cold regions engineering.

REFERENCES

ACPA (2008), “Frost-Susceptible Soils,” ACPA Concrete Pavement Technology Series TS204.3P, American Concrete Pavement Association.

Akagawa, S. (1988). “Experimental Study of Frozen Fringe Characteristics.” Cold Regions Science and Technology. Vol. 15, pp. 209-223

ASTM Standard D7099-04 (2010). “Standard Terminology Relating to Frozen Soil and Rock.” ASTM International, West Conshohocken, PA, DOI: 10.1520/D7099-04R10.

Dagli, D., Zeinali, A., Gren, P., and Laue, Jan. (2018). “Image Analyses of Frost Heave Mechanisms Based on Freezing Tests with Free Access to Water.” Cold Regions Science and Technology. Vol. 146, pp. 187-198

Holtz, R. D., Kovacs, W. D., and Sheahan, T. C. (2011). An Introduction to Geotechnical Engineering, 2nd edition. Prentice Hall.

Johnston, G. H (1981). PERMAFROST Engineering Design and Construction. John Wiley and Sons.

Kim, M., Seo, H., Lawson, W. D., and Jayawickrama, P. W. (2015). “Tangential Heave Stress for Design of Deep Foundations Revisited.” Proceedings of 16th International Conference on Cold Regions Engineering, Salt Lake City, Utah, July 2015, pp. 404-415

Kiselev, M. F. (1973). “Values of the tangential stresses of ground heave.” Proceedings of 2nd International Conference on Permafrost: USSR Contribution, National Academy of Sciences, Washington, D.C.

Nidowicz, B. and Shur, Y. L. (1998). “Russian and North American approaches to pile design in relation to frost action.” Permafrost – Proceedings of 7th International Conference, Yellowknife, Canada, Collection Nordicana No. 55, pp. 803-809.

Penner, E. (1986). “Aspects of Ice Lens Growth in Soils.” Cold Regions Science and Technology. Vol. 13, pp. 91-100

Pewe, T. L. and Paige, R. A. (1963). “Frost Heaving of Piles with and Example From Fairbanks, Alaska: A review of the principles of ice growth in the ground with special reference to its effect on piles” A final report submitted to United States Department of the Interior

State Building Committee. (1991). SNiP 2.02.04-88. Osnovaniya I fundamenti na vechnomerzlikh gruntakh (Foundations of buildings and structures on permafrost). Building standards and codes. State Building Committee, Moscow (in Russian)

Tsytovich, N. A. (1975). The Mechanics of frozen ground. Scripta Book Company, Washington, D.C.

U.S. Department of the Army and the Air Force. (1983). TM-5-852-4: Arctic and subarctic constructions for structures. Technical Manual, Department of the Army and the Air Force.

USDOD (2001), “Pavement Design for Airfields,” Unified Facilities Criteria, UFC 3-260-02, U.S. Department of Defense, 30 June 2001.

Xia, D. (2006). Frost Heave Studies Using digital Photographic Technique. MS thesis. University of Alberta, Edmonton, Alberta